THE ABUNDANCES OF LIGHT AND MEDIUM SIZE CLUSTERS IN LOW DENSITY NUCLEAR MATTER

تكون الأنوية الخفيفة والمتوسطة في المادة النووية قليلة الكثافة

By

WAAD ALI IKDEER AWAD

June, 2016

Thesis committee: Prof. Henry Jaqaman (Principal advisor)

Dr. Wafaa Khater (Member)

Dr. Hazem Abu Sara (Member)

This Thesis was submitted in partial fulfillment of the requirements for the Master's Degree in Physics from the Faculty of Graduate Studies at Birzeit University, Palestine
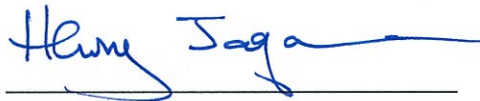
THE ABUNDANCES OF LIGHT AND MEDUIM SIZE CLUSTERS IN LOW DENSITY NUCLEAR MATTER

By

WAAD ALI IKDEER AWAD

Accepted by the Faculty of Graduate Studies, Birzeit University, in partial fulfillment of the requirements of the Master's Degree in Physics

Thesis committee:

_____

Henry Jaqaman Ph.D. (Principal advisor)

_____

Wafaa Khater Ph.D. (Member)

_____

Hazem Abu Sara Ph.D. (Member)

June, 2016

ACKNOWLEDGEMENT

I extend sincere thanks and appreciation to Prof. Henry Jaqaman for his continuous support and assistance from the outset until the final steps in this thesis. I would like also to thank the members of my advisory committee, Dr. Wafaa Khater and Dr. Hazem Abu Sara. I am also thankful for Ms. Arij Abdul-Rahman for her advices in the writing of this thesis and for all faculty members at the Department of Physics. My thanks and heartfelt appreciations also go to my family and friends.

ABSTRACT

The formation of nuclear clusters at low nuclear density has been investigated experimentally and theoretically over the last few years. It also has great interest in astrophysics and cosmology. At low density, nuclear matter can minimize its entropy and energy by forming clusters. Previous studies included the formation of clusters up to A=4, whereas our study includes the formation of clusters up to A=25. We study the effect of including these clusters on the critical temperature and the equation of state of low energy nuclear matter. The formation of the clusters is studied within the modified Nuclear Statistical Equilibrium Model (NSE) which assumes that the clusters are in chemical equilibrium with the nucleons in the surrounding vapor. The NSE is modified by including the decrease in the cluster's binding energy with increasing density of the surrounding medium of free nucleons. We find that these clusters affect the composition of nuclear matter significantly at different ranges of densities. Also including these clusters decrease critical temperature by several MeV's.

ملخص

كان تكون الأنوية الخفيفة في المادة النووية قليلة الكثافة موضوعا لعدة دراسات على مدى السنوات القليلة الماضية، ولهذا الموضوع أهمية في علم الفيزياء الفلكية وعلم الكونيات. فعندما تكون المادة النووية قليلة الكثافة فإنها تعمل على تقليل طاقتها بتكوين الأنوية. في الدراسات السابقة تم حساب نسبة تواجد هذه الأنوية التي تحتوي على 2- 4 نيوكليونات فقط. لكن في هذه الدراسة قمنا بحساب نسبة تواجد هذه الأنوية في المادة النووية قليلة الكثافة وبتضمين الأنوية التي يكون عددها الكتلي أقل أو يساوي 25 نيوكليون. وقمنا بدراسة تأثير وجود هذ الانوية على درجة الحرارة الحرجة وعلى معادلة الحالة للمادة النووية قليلة الكثافة. وذلك باستخدام صيغة معدلة من نموذج التوازن الاحصائي النووي الذي يفرض وجود اتزان كيميائي بين الأنوية والوسط المحيط. تتضمن الصيغة المعدلة المستخدمة من النموذج تناقص طاقة ربط الأنوية المتكونة بزيادة كثافة الوسط المحيط بها والمكون منا نيوكلونات حرة. لقد وجدنا أن الانوية التي تمتلك نيوكلونات مابين 4- 25 تتواجد بنسب لايمكن إهملها في المادة النووية على كثافات مختلفة، وتؤثر على درجة الحرراة الحرجة بحيث تقل عدة ميغاالكترون فولت.

TABLE OF CONTENTS

LIST OF FIGURES

LIST OF TABLES

CHAPTER1. INTRODUCTION

Studying the composition and properties of nuclear matter at various temperatures and densities is an important topic in nuclear physics. A related problem is the formation of clusters in very low density nuclear matter, which is the subject of many studies [1, 2, 3, 4, 5, 6]. The previous studies determined the composition of very low density nuclear matter by including free nucleons and clusters up to A=4.

Low density nuclear matter occurs in the envelope of expanding hot matter from heavy-ion collision and in the envelope of core collapse supernova. The formation of clusters changes the properties of nuclear matter and contributes to new reactions that control the dynamical evolution of stars [4]. The clusters are formed when the density of nuclear matter is much less than saturation density in order to minimize the energy of the system.

In this study, we consider the formation of the heavier clusters up to A=25 by using a modified form of the nuclear statistical equilibrium model (NSE) which assumes that the clusters are in chemical equilibrium with the surrounding vapor.

The binding energy of these clusters is affected by the surrounding medium. As the medium density increases the cluster's binding energy decreases and the cluster will dissolve into its constitutes nucleons at a certain density called the Mott density. This effect is not included in the nuclear

statistical equilibrium model (NSE) in it is original form, which considers the binding energy of the cluster to be independent of density.

The effect of the surrounding medium on the binding energy of the cluster is considered by assuming the binding energy to be density dependent.

Thermodynamically the system is represented by   the equation of state in which all the information about the system is encoded. In many studies [2, 3,4] low density nuclear matter equation of state was derived based on various models.

In 1982, Röpke et al investigated thermodynamic properties for a homogenous system of free nucleons and 'composite' particles (bound states of nucleons). They studied the abundance of deuterons imbedded in the surrounding nuclear matter by using the Bethe-Goldstone equation for thermodynamic Green functions [5].

After one year Röpke et al improved their work by taking into account the medium correlation in the equation of state. They also included clusters up to A=4 (deuterons, helions, tritons and alphas), but they neglected the difference between the helion binding energy and that of the triton [7].

In 1985, Levit and Bonche studied the stability of hot nuclei immersed in the vapor which they assumed to consist of nucleons. They showed that such nuclei can be heated up to a limiting temperature, and above this temperature the hot nucleus cannot exist as there is no solution representing the bound nucleus [8].

In 1989, Jaqaman [9] improved the equation of state considered by Levit and Bonche by considering asymmetric nuclear matter. In another study [10]

Jaqaman generalized the equation of state used in [9] by introducing the density-dependent nucleonic effective mass to investigate how it affects the stability of the hot nuclei. He also showed that considering the electric charge of the vapor will raise the value of the limiting temperature.

In 2004, Beyer et al studied the properties and distribution of light nuclei (up to A=4). The statistical model was used and the Hartree Fock (HF) approximation was introduced for quasi-particle energy. They found that the cluster binding energy depends on nuclear density, temperature and c.m. momentum [2].

After one year Röpke et al showed that light clusters with mass numbers A= 2, 3 and 4 are dominant in low density nuclear matter and so they must be included in any equation of state that describes the nuclear vapor at this limit [6].

In 2006, Horowitz and Schwenck presented the equation of state of low density nuclear matter consisting of protons, neutrons and alphas. They used nuclear statistical equilibrium (NSE) model to test its validity range, and then they used the virial expansion to consider the strong interaction. They showed that the alpha concentration decreases when the proton fraction decreases [3].

In 2008, Sumiyoshi and Röpke studied the abundances of light clusters up to A=4 in core-collapse supernova, within quantum statistical approach (unified the cluster and quasi-particle approach). They found that the deuteron and triton appear strongly in a wide region from the surface of the proto-neutron star (which

is a star that remains after supernova explosion; It is a tiny star with radius around 10 km and with extremely high density neutrons) in addition to ^{3}He and ^{4}He [11].

In 2009, Röpke in [12] studied the proprieties of light clusters (binding energy, mass, spin, Pauli blocking shift and root mean square (rms) charge radius) in dense nuclear matter. He used the Green function approach in different limits: first at low density limit where (NSE and virial) models are valid, second at high density limit where the relativistic mean field (RMF) model is valid and they suggested interpolating between the two limits. They studied nuclei up to A=4, but they predicted that the heavier nuclei will be important at low temperature and high density, so they avoided this region. They focused on the region where the abundance of heavier cluster is small, but in this study we will include the heavier clusters. They found when they included the medium modification the deviation from NSE model will start when the density is higher than 10^{-4} nucleons/fm^{3}.

In 2010, Typel et al studied the composition of nuclear matter at finite temperatures (T< 20MeV). The light clusters (up to A=4) were included and their dissolution at high density was considered. In this investigation two models were used: the Quantum Statistical (QS) model at the low density limit, which takes into account the modification of the cluster binding energy due to the Pauli blocking shift. The second model is relativistic mean filed model (RMF) which takes into account the relativistic effect. They found that α –particles are dominant at low temperatures. The abundance of clusters changes with increasing density of the medium such as the correlation between nucleons becomes more important. At higher temperatures above (4MeV) the deuteron is dominant at low

density (less than $10^{-2} \; nucleon/fm^3$) then, the three body bound states, helion and triton are the second dominant and finally the α –particle appears which will be less dominant at high temperature. Also they found in the QS model that deuterons dissolve faster with increasing density at fixed temperature than the heavier clusters (helion, triton and alpha). Whereas the alpha particle is the last cluster dissolves with increasing density at fixed temperature [4].

In a recent work Talahmeh and Jaqaman [13] calculated the limiting temperature for hot nuclei (assumed to be a liquid drop) in thermal, chemical and mechanical equilibrium with the surrounding vapor. The vapor was assumed to include not only nucleons but also clusters of nucleons up to A=4. They found that the limiting temperature was reduced by several MeV's when the clusters are included in the vapor equation of state.

This thesis is organized as follows: in chapter (2), we will study the equation of state of ideal quantum gases. In chapter (3), we will investigate the equation of state of a gas of nucleons interacting via the Skyrme force and its critical temperature. In chapter (4), we will review the Mott transition and in chapter (5), we will study the abundances of clusters up to A=25 by using the Nuclear Statistical Equilibrium model. In chapter (6), we will study the effect of including clusters on the equation of state of nuclear matter at low densities.

CHAPTER2. EQUATION OF STATE OF IDEAL QUANTUM GASES

The ideal quantum gas system describes a system of indistinguishable particles in which the interaction between the particles is negligible. These particles can be fermions or bosons. In thermodynamics such a system is described by finding a mathematical representation between the main variables of the system (volume, temperature and pressure) which is called the equation of state (EOS) of the system. In this chapter we will discuss the properties of fermions and bosons and investigate the equation of state of an infinite system composed of non-interacting fermions or bosons.

2.1. EQUATION OF STATE I FOR DEAL FERMI GAS

Nuclear matter is composed of nucleons that can be either protons or neutrons. The proton differs from the neutron by having a positive electric charge. When we neglect the charge of the proton, we can say that the proton and neutron are two states of the same particle (the nucleon) with mass $\approx 940 \ MeV$. Nucleons have spin ½ and therefore are classified as fermions, so they obey Fermi-Dirac statistics. As a result   nucleons cannot occupy the same quantum- mechanical state [14].

The probability density or the mean occupation number for an ideal Fermi gas which gives the probability that a certain energy level is occupied at temperature T [15]:

$$n_i = \frac{1}{exp(\beta(\varepsilon_i - \mu)) + 1} \tag{2.1}$$

where ε_i is the single particle energy. μ is the chemical potential and it has energy unit and $\beta = 1/T$. T is the temperature in MeV where $T = k_b t$. Here t is the temperature in Kelvin and k_b is the Boltzmann constant $k_b = 8.617 \times 10^{-11}$ (MeV/K). A temperature T=1 MeV is equivalent to $1.1 \times 10^{10} K$.

The derivation of the pressure and chemical potential equation of state for an infinite system of non-interacting fermions was determined by Talahmeh and Jaqaman in [13] using Fermi-Dirac statistics and the canonical partition function: The energy (ε_k) of each fermion in this case is just the kinetic energy $\varepsilon_k = \frac{\hbar^2 k^2}{2m}$ where k is the wave number of the particle and is equal the inverse of the wave length multiplied by 2π. The canonical partition function $Q(\beta) = \frac{V}{\lambda_T^3}$, where $\lambda_T = \left(\frac{2\pi\hbar^2}{mT}\right)^{\frac{1}{2}}$ is the mean De Broglie wavelength of the gas particle in the ideal gas evaluated at temperature T and V is the volume of the ideal gas.

The chemical potential and the pressure for an ideal Fermi gas can be written as [13]:

$$\mu(T, \rho_{free}) = T\left(ln\left(\frac{\lambda_T^3 \rho_{free}}{g}\right) + \sum_{n=1}^{\infty} b_n \left(\frac{\lambda_T^3 \rho_{free}}{g}\right)^n\right) \tag{2.2}$$

$$P = T\left(1 + \sum_{n=1}^{\infty}\left[\left(\frac{n}{n+1}b_n\right)\left(\frac{\lambda_T^3 \rho}{g}\right)^n\right]\right) \tag{2.3}$$

where $g = 4$ represents the spin-isospin degeneracy of the nucleon. The b_n coefficients are calculated up to $n = 9$ by using mathematica and the method is described in [9]. The results are illustrated in Table1.

Table 1: Numerical values of the b coefficients calculated for the ideal Fermi gas

	b_n	$\left(\frac{n}{n+1}\right)b_n$
n=1	0.3535533905933	0.1767766952966
n=2	-0.0049500897299	-0.0033000598199
n=3	$1.483857713 \times 10^{-4}$	$1.112893285 \times 10^{-4}$
n=4	$-4.4256301 \times 10^{-6}$	$-3.5405041 \times 10^{-6}$
n=5	1.006362×10^{-7}	8.38635×10^{-8}
n=6	-4.272×10^{-10}	-3.662×10^{-10}
n=7	-1.17494×10^{-10}	$1.0280725 \times 10^{-10}$
n=8	7.93555×10^{-12}	7.05382×10^{-12}
n=9	-2.99582×10^{-13}	2.696238×10^{-13}

We will study the convergence of the series sum in equation (2.3) at different temperatures, to see when we can stop the sum because adding more terms has a negligible effect.
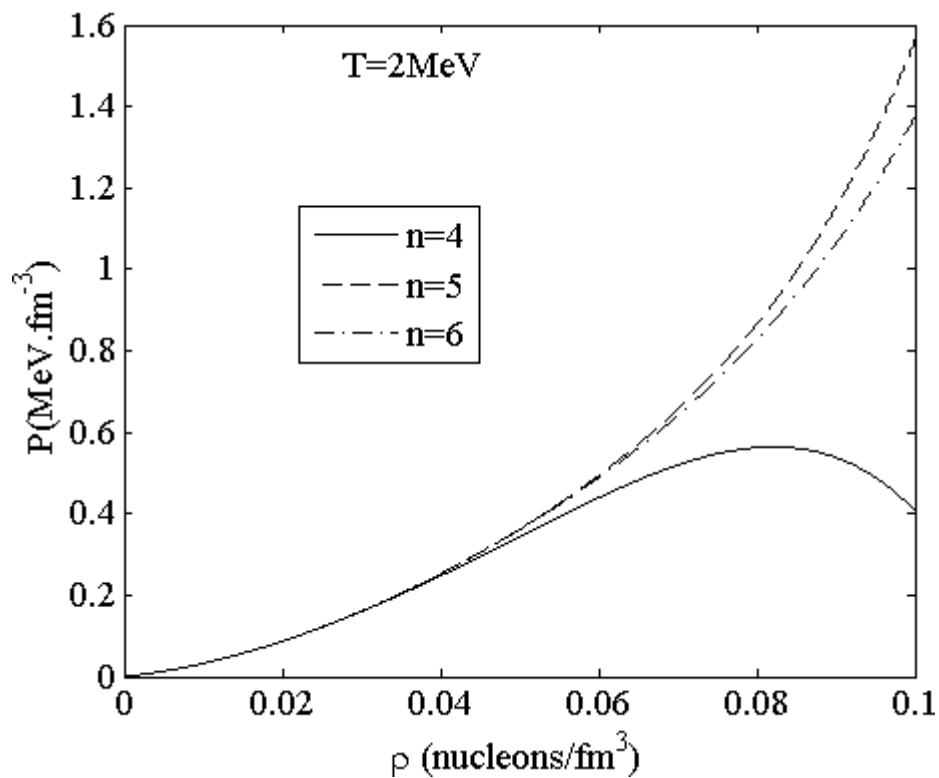
Fig.2.1. The pressure of an ideal Fermi gas of nucleons at T=2MeV

At temperature $T = 2MeV$ the pressure series does not converge at high density as seen in Fig.2.1. But at higher temperature the series converges. This kind of series is called an asymptotic series. Usually the series summation is stopped at the lowest term (This sentence is not clear, what do you mean by lowest term). In this series the lowest term occurs when n=6 [17]. Neglecting the higher b_n terms causes computational error. This error is negligible as the temperature increases as the b_n terms get smaller and smaller with density increasing. So the series will converge by adding the first few terms.
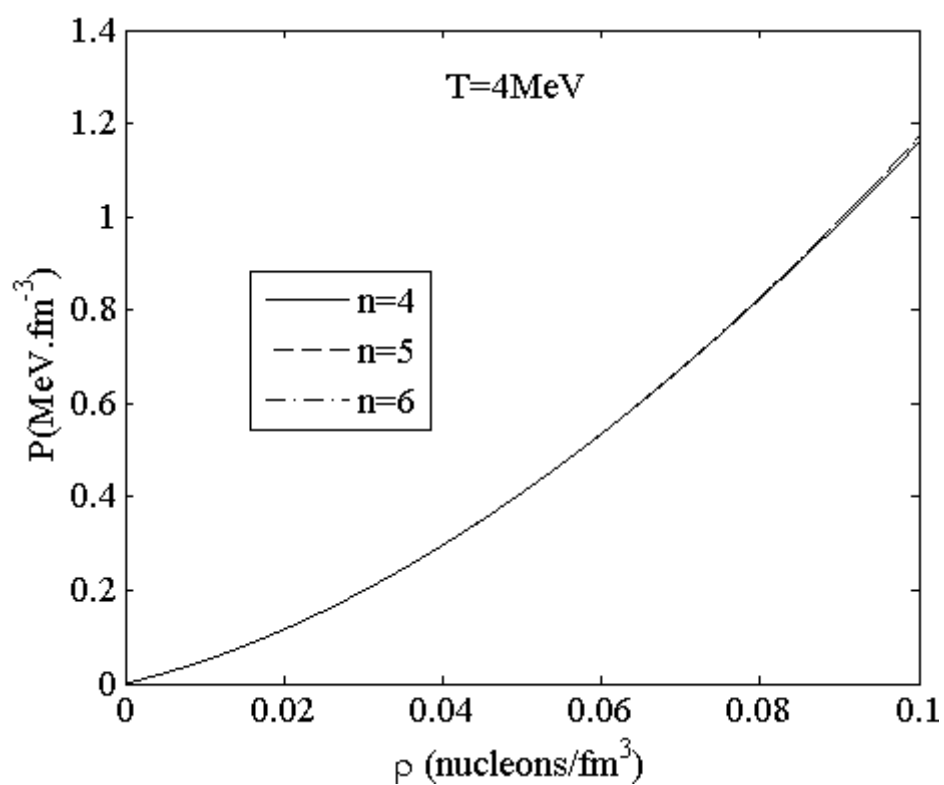
Fig.2.2. The pressure of an ideal Fermi gas of nucleons at T=4MeV
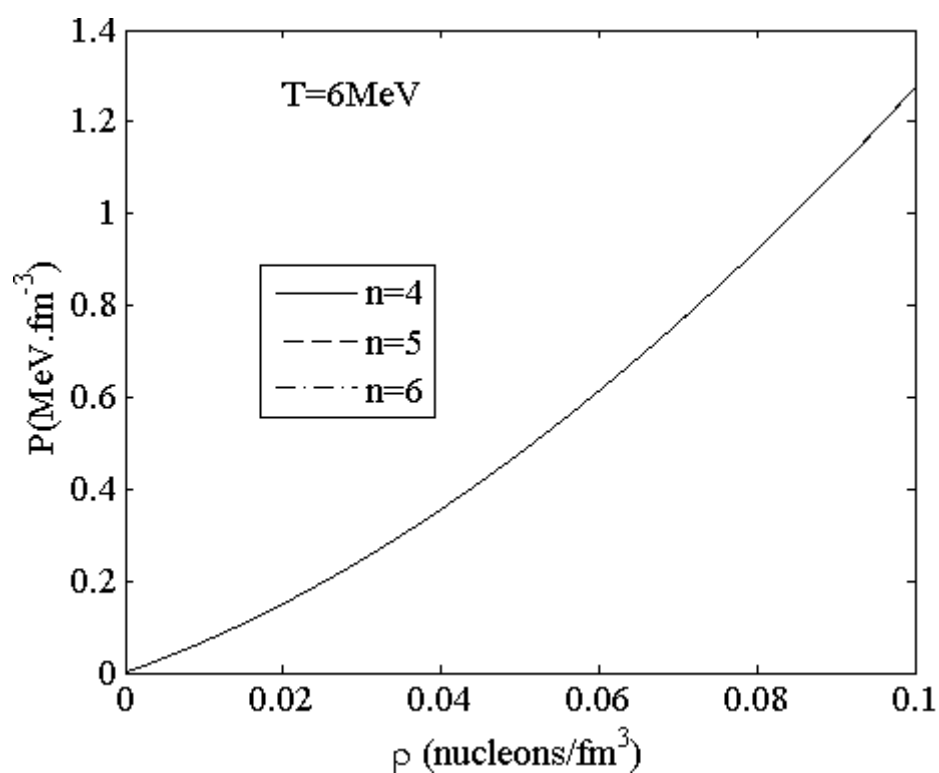
Fig.2.3. The pressure of an ideal Fermi gas of nucleons at T=6MeV.

As shown in Fig.2.1 which is at temperature T = 2MeV the pressure series converges for all densities up to $= 0.07\ nucleons/fm^3$. We note from Fig 2.2 and Fig 2.3 that the series converges up to $\rho = 0.1\ nucleons/fm^3$ at temperatures higher than 4MeV and therefore, we only need to sum the series up to n=6. We will see that, we will not need in our present work to go to higher densities (above $\rho = 0.1\ nucleons/fm^3$).

2.1. EQUATION OF STATE FOR IDEAL BOSE GAS

The free nucleons are classified as fermions, the nucleons can be found in bound states called nuclei. The nuclei can be fermions or bosons depending on the number of nucleons in the nucleus. If the number of nucleons is odd which means the spin of the nucleus is half integer then the nucleus is a fermion, but when the number of nucleons is even the total spin of the nucleus will be integer. In this case the nucleus will be a boson, The Bose-Einstein distribution is given by:

$$n_i = \frac{1}{exp(\beta(\varepsilon_i - \mu)) - 1} \tag{2.4}$$

The derivation of the chemical potential and pressure for an infinite system of non-interacting bosons is done in [13]:

$$\mu(T, \rho) = T\left(ln\left(\frac{\lambda_T^3 \rho}{g}\right) + \sum_{n=1}^{\infty} d_n \left(\frac{\lambda_T^3 \rho}{g}\right)^n\right) \tag{2.5}$$

$$P = T\left(1 + \sum_{n=1}^{\infty}\left[\left(\frac{n}{n+1} d_n\right)\left(\frac{\lambda_T^3 \rho}{g}\right)^n\right]\right) \tag{2.6}$$

where g is the spin degeneracy factor. The d_n coefficients are related to $b_n$coefficients (given in Table 1) by the relation:

$$d_n = (-1)^n b_n \tag{2.7}$$

To investigate the behavior of an ideal Bose gas, we plot the pressure of non-interacting alpha particles. The spin of the alpha particle is zero, so the spin degeneracy factor $g = 2s + 1 = 1$ for the alpha particle.

The convergence of the pressure series of non-interacting bosons is shown in Fig 2.4 and Fig.2.5 where the bosons are alpha particles. It can be seen for non-interacting bosons the series converges faster than the case of non-interacting fermions. We can note that by comparing Fig.2.4 by Fig.2.2. The series converges up to densities around $\rho = 0.1 \ alphas/ fm^3$ in the case of alpha particles at temperature $T = 2 \ MeV$ as illustrated in Fig.2.4. Whereas in the case of nucleon the pressure series converges around up to densities around $\rho = 0.07 \ nucleons/ fm^3$ as illustrated in Fig.2.2. For higher temperatures, we note that for $T = 4MeV$ and $T = 6MeV$ the pressure series converges up to density reaches $\rho = 0.2 \ alphas/fm^3$ as illustrated in Fig.2.5 and Fig.2.6.
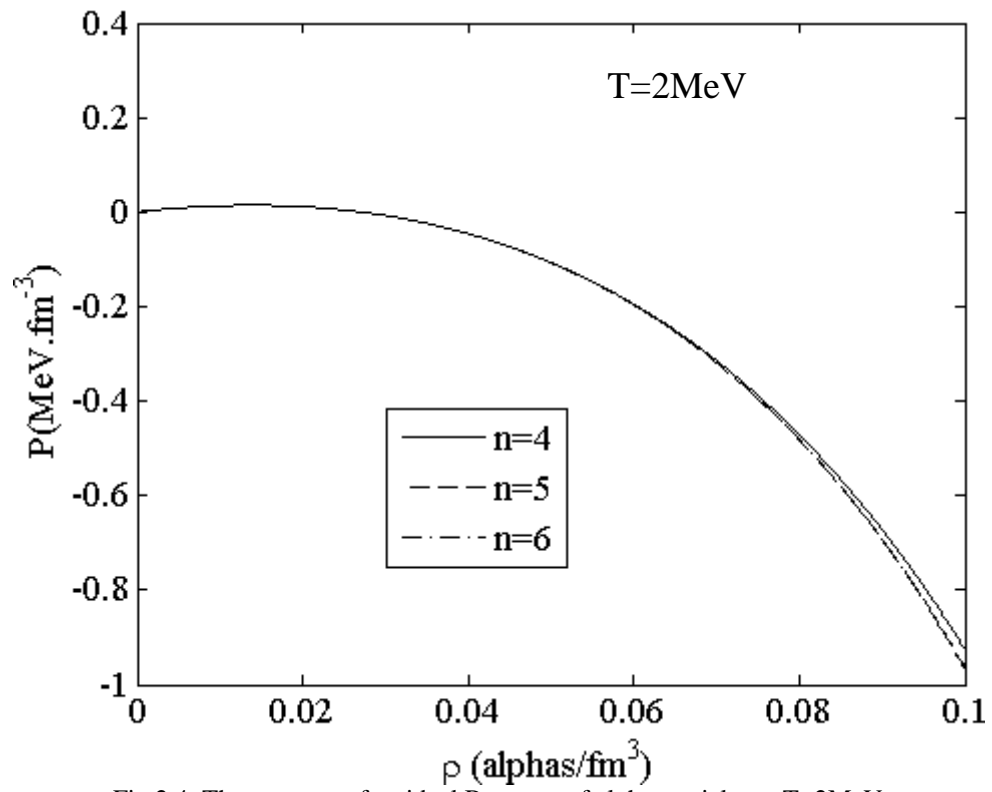
Fig.2.4. The pressure of an ideal Bose gas of alpha particles at T=2MeV
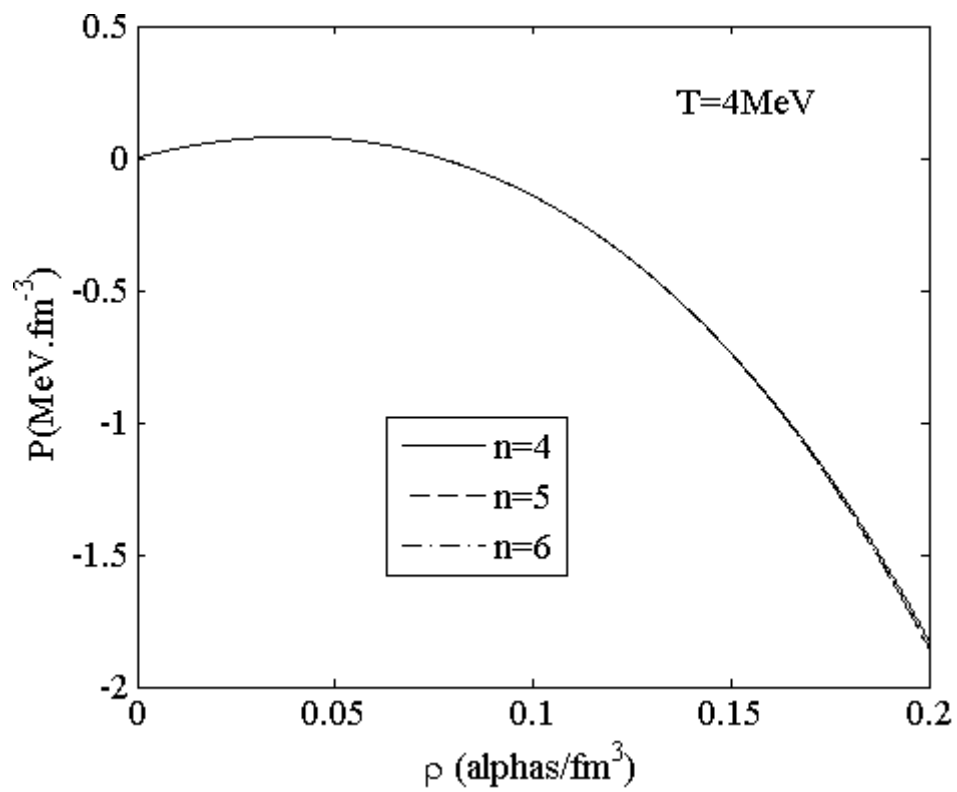
Fig.2.5. The pressure of an ideal Bose gas of alpha particles at T=4MeV

We note that the pressure of non-interacting alpha particles differs from non-interacting nucleons. If we compare both Fig.2.6 and Fig.2.3 at low density limit $\rho < 0.1 \ nucleons/fm^3$, we see that the pressure of free nucleons at T= 6MeV is always increasing with density and it is positive, but for system of non-interacting alpha particles the pressure first increases then decreases at higher densities (in Fig.2.6).

This reflects the phenomenon of Bose-Einstein condensation which occurs at low enough temperatures or high enough densities when all bosons are pushed down to the ground state. This is attributed to the infinite occupancy of the ground state of a Bose gas. This does not occur in Fermi systems because of the Pauli Exclusion Principle.
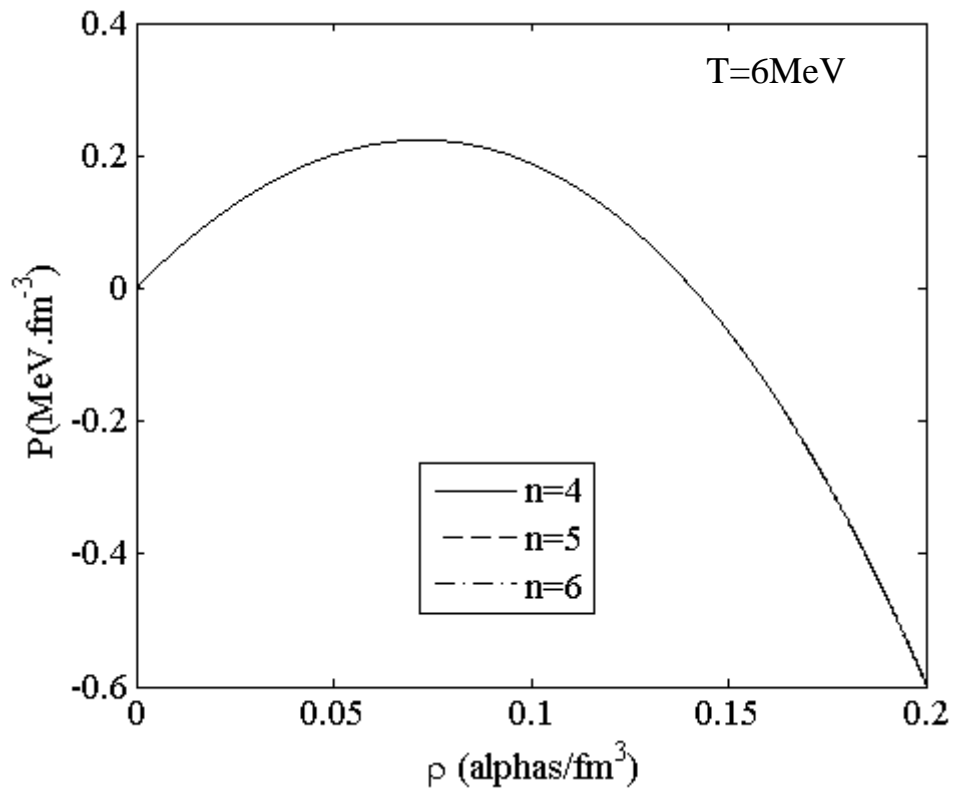
Fig.2.6. The pressure of an ideal Bose gas of alpha particles at T=6MeV

In studying the equation of state (EOS) of any nuclear system we need to identify the constitutes of the system if they are fermions or boson. We will handle this in chapter 6 when we will study the pressure equation of state of clustered nuclear matter.

CHAPTER 3. EQUATION OF STATE OF AN INFINITE GAS OF INTERACTING NUCLEONS

In chapter 2 we studied the pressure and chemical potential equation of state for a system of non-interacting fermions and bosons. Actually nucleons interact with each other via the nuclear force regardless of their charge, and the protons interact with each other via the Coulomb force (which will be ignored in this chapter).

3.1. SKYRME MODEL

Many attempts were made to investigate the interaction between nucleons. The force between nucleons is affected by the surrounding medium [16]. The effective forces used to describe the interaction between nucleons can be either density dependent or independent. The density independent forces have difficulties in determining the nuclear radii, the binding energy, and the single particle density of heavy nuclei, whereas the density dependent forces give a fair description for these properties. Among these forces is the Skyrme force which was first proposed by Skyrme in 1959 [21]. The Skyrme interaction is a density-dependent zero-range effective nucleon-nucleon interaction and was successfully used by Vautherin and Brink [16] in their study of the properties of nuclear matter and some closed-shell nuclei. We will use the two -body Skyrme interaction:

$$V_{12} = -t_0 \delta(\vec{r}_1 - \vec{r}_2) + \frac{1}{6} t_3 \rho^\sigma \left[\frac{\vec{r}_1 + \vec{r}_2}{2} \right] \delta(\vec{r}_1 - \vec{r}_2) \tag{3.1}$$

where $\vec{r}_1, \vec{r}_2$ are the position vectors of the two nucleons relative to a reference point. ρ is the total nuclear matter density and the parameter σ is used to control the incompressibility of nuclear matter without changing its binding energy. $t_0\ and\ t_3$ are the Skyrme interaction parameters. These parameters can be determined phenomenologically by fitting the ground state properties of nuclear matter.

In [16] the Skyrme interaction parameters were adjusted to fit the binding energy and density of nuclear matter. We consider the nuclear matter symmetric so the number of protons is equal to the number of neutrons. Also we neglect the Coulomb force between protons.

Equation (3.1) was used in [13] by Talahmeh and Jaqaman to derive the equation of state of symmetric nuclear matter, which will be discussed in the next section of this chapter. In Table 2, we illustrate the Skyrme parameters that were used in [9]. The incompressibility is a measure of the relative volume change of a fluid or solid when pressure is changed. A general definition of the incompressibility is given by:

$$K = -\frac{1}{V}\frac{\partial P}{\partial V} \qquad\qquad (3.2)$$

where V is the volume and P is the pressure of the nuclear matter. The minus sign ensures that the incompressibility is always a positive quantity. The values of K at different σ is shown in Table 2.

The relations that connect the parameters in (3.1) with those in Table 2 are as follows [9]:

$$a_0 = \frac{3}{8} t_0 \tag{3.3}$$

$$a_3 = \frac{1}{16} t_3 \tag{3.4}$$

$$\sigma = \frac{(K - 9E_B - E_K)}{(9E_B + 3E_K)} \tag{3.5}$$

$$a_0 \rho_0 = \left[(1 + \sigma)E_B + \left(\sigma + \left(\frac{1}{3} \right) \right) E_K \right] / \sigma \tag{3.6}$$

$$a_3 \rho_0^{1+\sigma} = (E_B + E_K/3)/\sigma \tag{3.7}$$

E_B is the nuclear matter binding energy per particle. E_K is the nuclear matter kinetic energy per particle. K is the nuclear incompressibility. The incompressibility of a nucleus can be calculated from the energy required to excite a nucleus without changing its shape. When a nucleus acquires an excess of energy (example of that Coulomb excitation due to charged particle passing near from the nucleus) it can be set into vibration around its equilibrium shape. The volume is now changing (the nucleus remains spherical but its radius vibrates) while the total amount of nuclear matter remains constant. This is called the breathing mode [14]. ρ_0 is the saturation density or the density of nuclear matter that is distributed uniformly in the interior of a heavy nucleus of large radius. The value of ρ_0 is inferred from the maximum density of finite nuclei, the commonly used value is: $\rho_0 = 0.17 \; nucleons/fm^3$ [8, 9, 10].

Table 2: Skyrme interaction parameters [9]

	x_0	$a_0\rho_0$ (MeV)	$a_3\rho_0^{1+\sigma}$ (MeV)	K (MeV)
$\sigma = 0.25$	0.75	136	96	222
$\sigma = 1$	0.47	64	24	384

3.2. EQUATION OF STATE INCLUDING SKYRME INTERACTION

In chapter 2, we investigated the equation of state for a system of non-interacting nucleons; the single particle energy in this case is just the kinetic energy. Now, we want to investigate a system of interacting nucleons which interact via the Skyrme force only.

The single particle energy which is used in this thesis was investigated in [16] and has the general form:

$$\varepsilon_q = \frac{\hbar^2 k^2}{2m_q} - t_0\left[\left[1 + \frac{x_0}{2}\right]\rho - \left[x_0 + \frac{1}{2}\right]\rho_q\right]$$

$$+ \frac{1}{4}t_3\left[\rho^{1+\sigma} - \sigma\rho^{\sigma-1}\rho_q^2 + (\sigma - 1)\rho^\sigma\rho_q\right] + \delta_{pq}V_{Coul}(\rho)$$

(3.8)

As we assumed in the previous section the nuclear matter is symmetric, so the number of neutron (n) equal the number of protons (p). ρ_q denotes ρ_n or ρ_p

because the nuclear matter is symmetric the densities of protons and neutron are equal $\rho_p = \rho_n = \frac{\rho}{2}$. Also we neglect the Coulomb term, so we set it to zero. Equation (3.8) will be:

$$\varepsilon = \frac{\hbar^2 k^2}{2m} + \varepsilon_0 \qquad (3.9)$$

where $\varepsilon_0 = -\frac{3}{4} t_0 \rho + \frac{t_3}{8}\left(1 + \frac{\sigma}{2}\right)\rho^{1+\sigma}$.

The pressure and chemical potential equations of state for symmetric nuclear matter, when including the Skyrme interaction were derived by Jaqaman in [10]:

$$\tilde{P}(T,\rho) = -a_0\rho^2 + a_3(1+\sigma)\rho^{(2+\sigma)} + T\rho\left[1 + \sum_{n=1}^{\infty}\frac{n}{n+1}b_n\left[\frac{\lambda_T^3\rho}{g}\right]^n\right] \qquad (3.10)$$

$$\tilde{\mu}(T,\rho) = -2a_0\rho + a_3(2+\sigma)\rho^{(1+\sigma)} + T\left[ln\left[\frac{\lambda_T^3\rho}{g}\right] + \sum_{n=1}^{\infty}b_n\left[\frac{\lambda_T^3\rho}{g}\right]^n\right] \qquad (3.11)$$

where g=4 is the spin- isospin degeneracy factor. Equation (3.10) is plotted in Fig. 3.1 at four different temperatures using the force with σ=0.25. We note from Fig. 3.1 that each pressure isotherm consists of three regions: the low-density vapour region where the pressure increases with density, the intermediate-density region (the negative slope region) where the system is unstable mechanically (unphysical region) and the liquid high-density region. Above the critical temperature the nuclear matter will be in a single fluid phase.
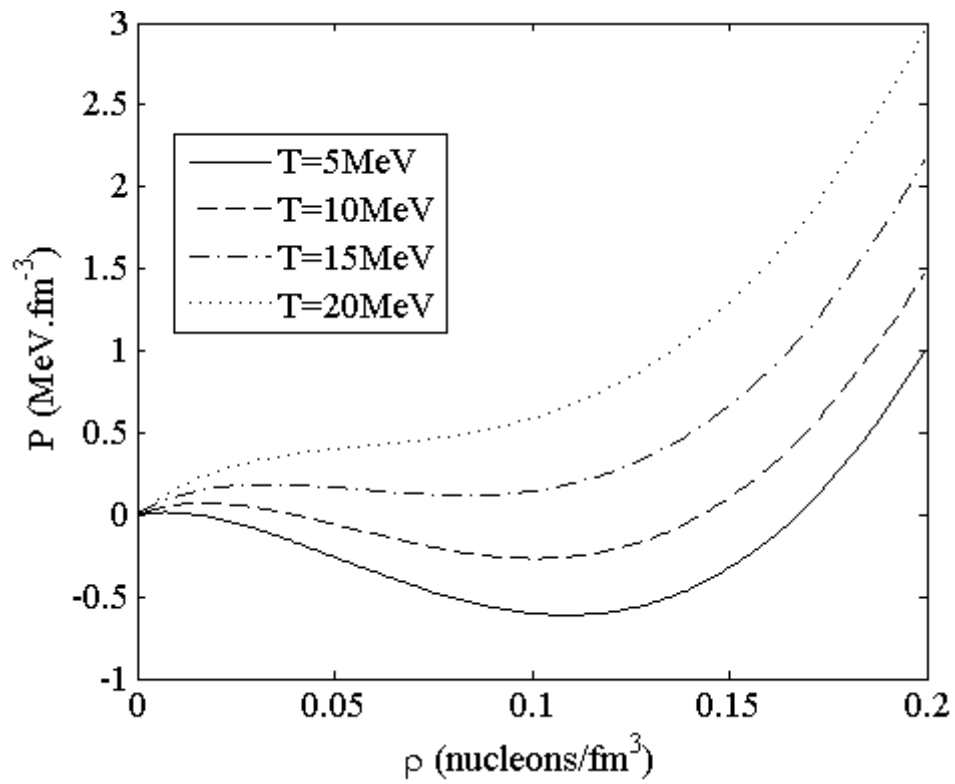
Fig. 3.1. The pressure isotherms of a system of nucleons interact via Skyrme force at four different temperatures

We see from Fig 3.1 that the pressure isotherms rise to maximum then drop to minimum then rise again for T=5MeV, T=10MeV and T=15MeV. But at T=20MeV the pressure isotherm is increasing and the minimum and maximum have disappeared which means the system is above the critical temperature, The critical point is the point at which the isotherm has an inflection point (at which the curve has a zero curvature).
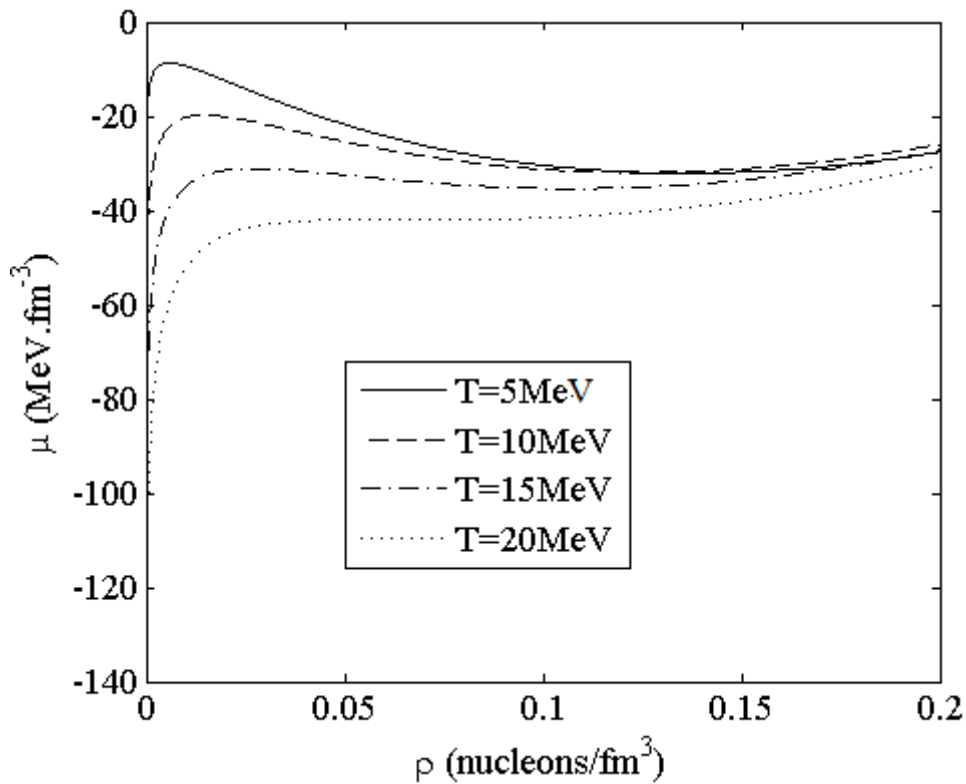
Fig.3.2. The chemical potential isotherms of a system of nucleons interact via Skyrme force at four different temperatures.

Equation (3.11) is plotted in Fig.3.2. The chemical potential isotherms increase until they reach a maximum. Then they decrease to a minimum and then again increase with density. At the critical temperature the minimum and maximum will merge and we have an inflection point. Above the critical temperature the slope is always positive. We will demonstrate this in the next section.

3.3. THE CRITICAL TEMPERATURE

Above the critical temperature the nuclear matter will be in a single fluid phase. We see from Fig 3.1 and Fig 3.2 the pressure and chemical potential isotherms rise to maximum and then drop to minmum. When the maximum and minimum merge the temprature is the crtical one. The critical temprature of an infinte system of interacting nucleons is determined in [9,13,17].

The critical temprature can be obatained from the pressure or chemical potential isotherms by determining the inflection point:

$$\frac{dP}{d\rho} = \frac{d^2P}{d\rho^2} = 0 \quad \text{if we obtained it from a plot of pressure isotherms}$$

or

$$\frac{d\mu}{d\rho} = \frac{d^2\mu}{d\rho^2} = 0 \quad \text{if we obtained it from a plot of chemical potential isotherms.}$$

We investigated the critical temperature for a system of nucleons interacting via the Skyrme force by plotting the pressure isotherms at different temperatures. From the graph, we identify where the inflection point occurs, so we got the critical temperature is 17.3MeV for the Skyrme force with $\sigma = 0.25$ as seen in Fig.3.3. In the same manner, we can identify the critical point which includes (temperature, chemical potential and density) from the graph of chemical potential isotherms.
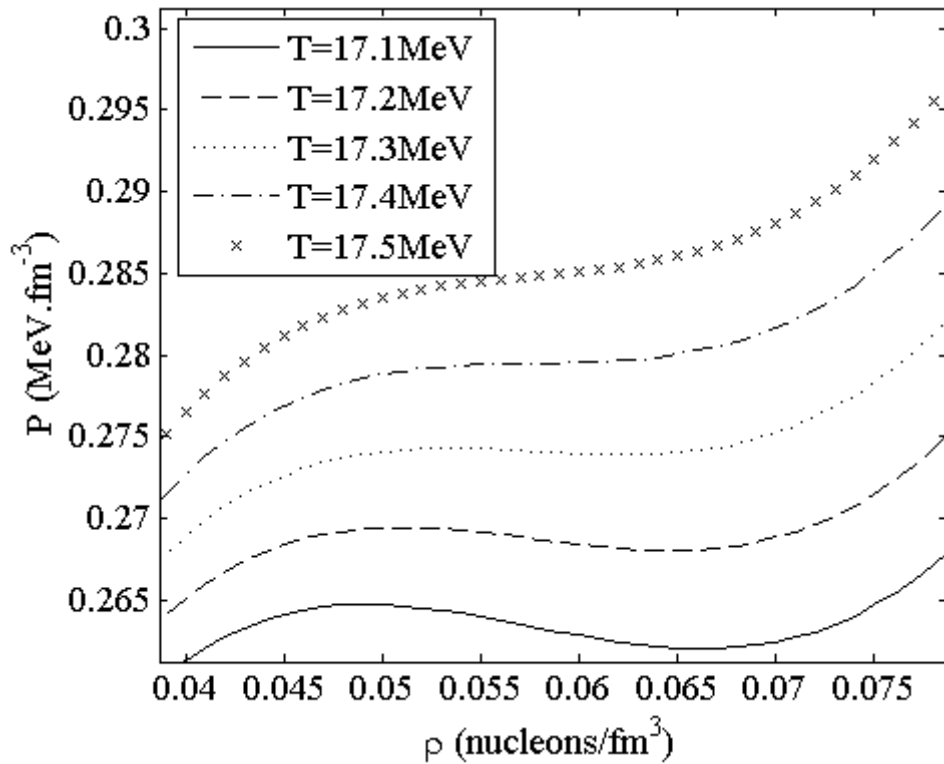
Fig.3.3. The determination of the critical temperature from the pressure isotherms for σ=0.25

Table 3 summarizes the critical temperature and density for an infinite system of nucleons interacting via the Skyrme force. The small difference in the values in different references is due to the number of terms considered in the series summation of the equation of state. In [13] summing is carried up to $n = 6$ while in [9, 17] the summing is stopped at $n = 5$. In Chapter 6, of the present work, we will investigate the critical temperature for nuclear matter consists of nucleons and clusters.

Table 3: summarizes the critical values at different σ values.

σ –parameter	$\sigma = 0.25$ [13]	$\sigma = 0.25$ [9]	$\sigma = 1$ [13]	$\sigma = 1$ [17]
$T_{critical}$ (MeV)	17.3	17.22	22.9	22.9
$\rho_{critical}$ (nucleons/fm^3)	0.0535	0.0602	0.064	0.068

CHAPTER4. THE MOTT TRANSITION

The properties of clusters are affected by the surrounding medium; by increasing the density of the medium the binding energy of the cluster will decrease. When the density of the medium reaches a certain value, the binding energy of the cluster becomes zero. This means that the cluster dissolves to its constituents .This density is called the Mott density. Each cluster has its own Mott density.

The dissolution of a cluster (Mott transition) occurs at the Mott density. The Mott density for light clusters up to (A=4) is calculated in several studies [4, 18, 19]. In [4] Typel calculated the Mott density for deuterons, helions, tritons and alphas. The calculation was based on the relativistic mean field (RMF) model and the Pauli blocking effect was considered. He neglected the coulomb energy and the cluster momentum relative to the medium.

The Pauli blocking effect is due to the indistinguishability between the nucleons inside the clusters and the free nucleons outside in the surrounding medium. The total wave function of the system must be antisymmetric under the exchange of any two nucleons not just the nucleons inside the cluster but also the exchange between a nucleon inside the cluster and a nucleon in the surrounding vapour [18].

In chapter 5 we will use the Mott densities for alphas, tritons, helions and deuterons to investigate the abundances of light clusters in the nuclear vapour. We will depend on the values which were calculated by Typel in [4].

The total binding energy of each cluster will be:

$$B_i = B_i^0 + \Delta B_i \qquad (4.1)$$

where B_i^0 is the binding energy of cluster i at zero density and ΔB_i is the binding energy shift. The results obtained by Typel in [4] for the binding energy as a function of the medium density are plotted at four different temperatures for the deuteron in Fig.4.1.
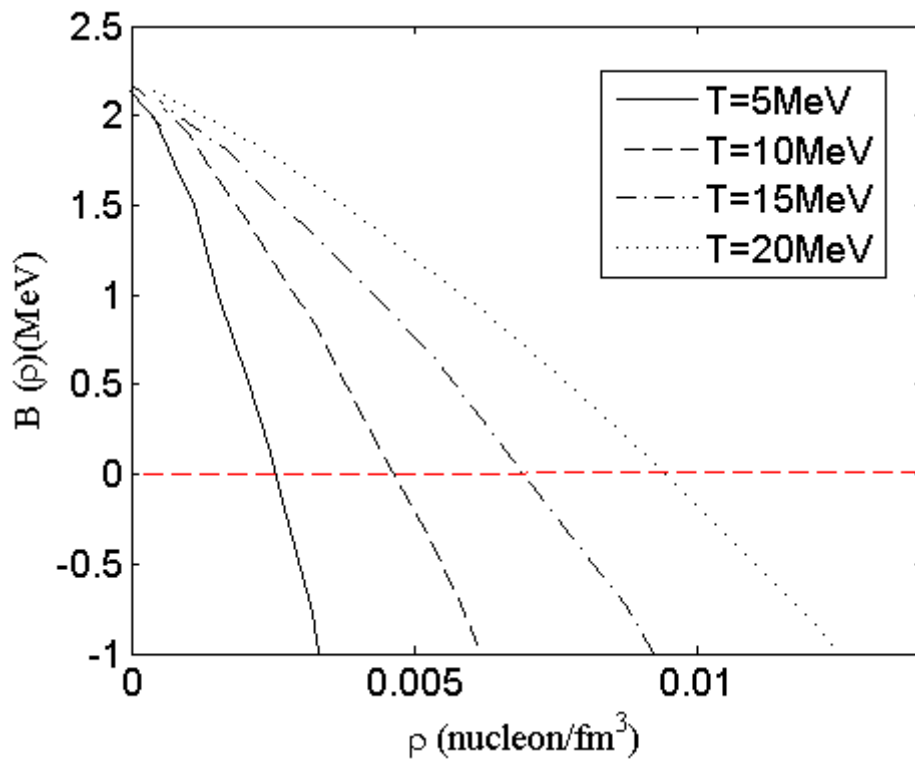
Fig.4.1. The deuteron binding energy as a function of density at four different temperatures as obtained by Typel [4] the red dashed line shows the zero energy point.

.

The red dashed line intersects the binding energy at zero point, which represents the Mott density for deuteron at temperatures 5, 10, 15 and 20MeV.

Typel in [4] assumed the clusters were at rest, the effect of the center of mass (CM) motion was considered in [18] for clusters up to A=4. They found that the value of the Mott density for light clusters increases when the (CM) motion is included. In this study, we depend on the Typel results about the Mott density for clusters up to A=4.

4.1. MOTT DENSITY FOR CLUSTERS UP TO A=4

Depending on the shift of binding energy due to the medium effects in [4], we extract the Mott-density of (alpha, hellion, triton and deuteron) from the results of Typel [4] for the binding energy versus the density at different temperatures. The values of the Mott densities for A=2-4 are summarized in Table 4 which will be used in our calculation in chapter 5.As seen in Table 4 the Mott density is just known for alpha, deuteron, helion and triton at different temperatures.

Table 4: Mott densities for various clusters at typical temperatures

	Deuteron	**Triton**	**Helion**	**Alpha**
T=2MeV	0.00148 fm^{-3}	0.0028 fm^{-3}	0.0023 fm^{-3}	0.0059 fm^{-3}
T=4MeV	0.00216 fm^{-3}	0.0036 fm^{-3}	0.0031 fm^{-3}	0.0073 fm^{-3}
T=5MeV	0.0025 fm^{-3}	0.0040 fm^{-3}	0.0035 fm^{-3}	0.0080 fm^{-3}
T=6MeV	0.0029 fm^{-3}	0.0046 fm^{-3}	0.0040 fm^{-3}	0.0088 fm^{-3}
T=8MeV	0.0038 fm^{-3}	0.0058 fm^{-3}	0.0052 fm^{-3}	0.0106 fm^{-3}
T=10MeV	0.0047 fm^{-3}	0.0069 fm^{-3}	0.0064 fm^{-3}	0.0123 fm^{-3}
T=15MeV	0.007 fm^{-3}	0.00964 fm^{-3}	0.00956 fm^{-3}	0.0167 fm^{-3}
T=20MeV	0.0093 fm^{-3}	0.0124 fm^{-3}	0.0125 fm^{-3}	0.0208 fm^{-3}

4.2. MOTT DENSITY FOR CLUSTERS WITH A>4

The Mott density is not known for clusters having A>4.We can determine the Mott densities for clusters with A>4 by extrapolating their values from the Mott densities values of the clusters having A=2–4. We plot the known cluster Mott densities versus the mass number of each cluster. For each temperature, we fit the data of known Mott densities (alpha, triton, helion and deuteron) by a quadratic polynomial as shown in Fig.4.2 at $T = 6MeV$. Equation (4.3) represents the Mott density as a function of the cluster mass number (A) at T =6MeV.

$$\rho_{Mott} = 0.0012 * A^2 - 0.0045 * A + 0.007 \qquad (4.3)$$

Then, we extrapolate the Mott density to heavier clusters from the graph as shown in Fig.4.3 at $T = 6MeV$. After that, we extract the Mott density of each type of cluster from the extrapolated graph. In the same way, we extrapolate the Mott density for each type of cluster at different temperatures.
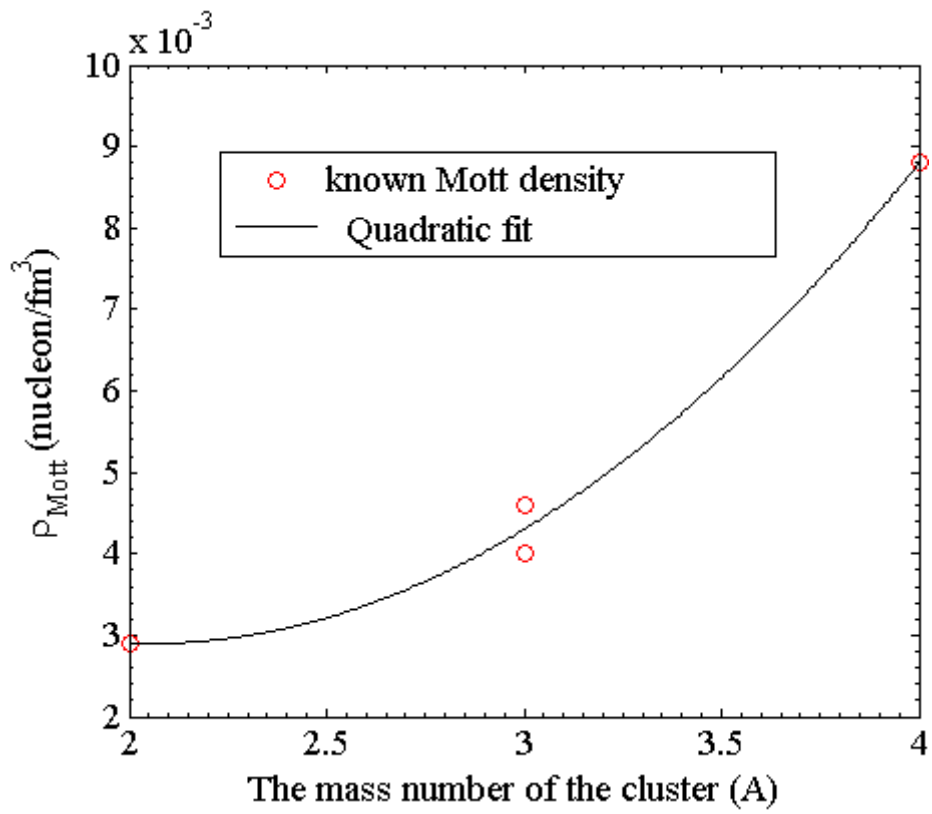
Fig.4.2. The Mott density of various clusters at T=6MeV.

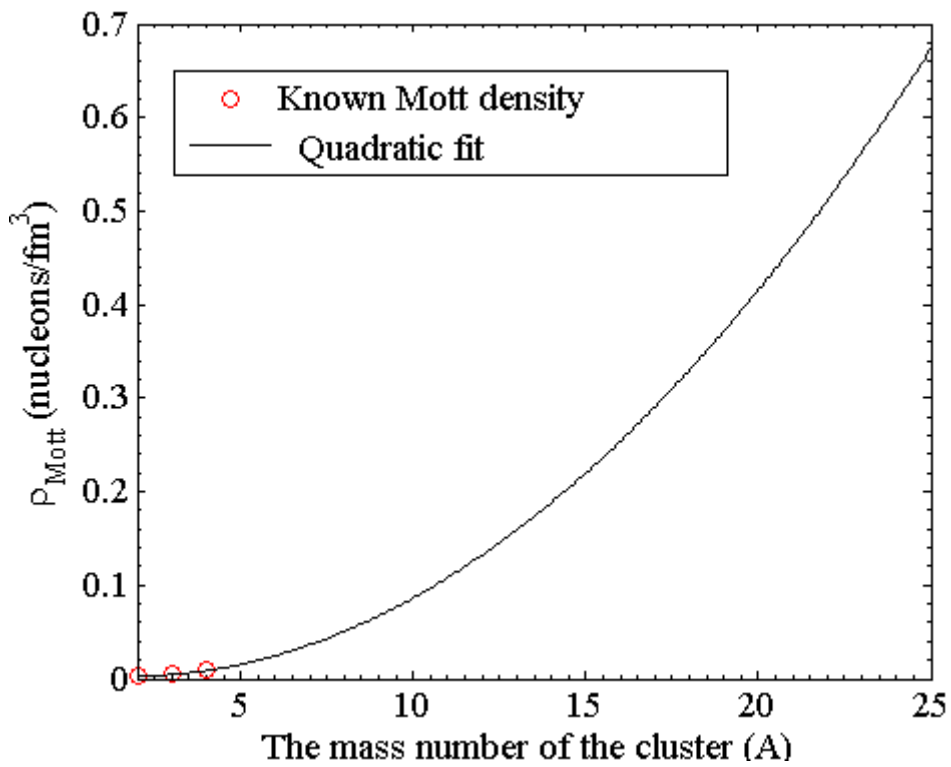**Fig.4.3.** The extrapolated Mott density of various clusters at T=6MeV.

CHAPTER5. NUCLEAR STATISTICAL EQUILIBRIUM MODEL

Including clusters in the equation of state of the nuclear matter has been the subject of many theoretical investigations [4, 10]: virial expansion, microscopic quantum statistical (QS) approach, relativistic mean filed (RMF) approach and nuclear statistical equilibrium (NSE) model.

5.1. REVIEW OF THE EQUATION OF STATE OF CLUSTERED NUCLEAR MATTER IN VARIOUS MODELS

Now, we will review the theoretical approaches that were used to get the equation of state of clustered nuclear:

5.1.1. THE MICROSCOPIC QUANTUM STATISTICAL APPROACH

The microscopic quantum statistical approach is a non-relativistic model that treats the clusters in nuclear matter as quasi-particles, it takes into account all of the interactions between the nucleons. The medium effect is considered in this model and its effects in forming and dissolving the clusters. In such manner the energy of quasi-particle will be in this form [4, 20]:

$$E_{A.Z}^{qu}(P) = E_{A,Z}^{(0)} + \frac{P^2}{2Am} + \Delta E_{A,Z}^{SE}(P) + \Delta E_{A,Z}^{Pauli}(P) + \Delta E_{A,Z}^{Coul}(P) + \cdots \quad (5.1)$$

where m is the mass of the nucleon, and P is the momentum of the cluster. The five terms of Eq. (4) are explained as follows:

$E_{A,Z}^{(0)}$ is the cluster binding energy in vacuum. $\frac{P^2}{2Am}$ is the kinetic energy of the cluster. $\Delta E_{A,Z}^{SE}(P)$ is the self energy shift due to all of the interaction between the cluster and other clusters and nucleons. $\Delta E_{A,Z}^{Pauli}(P)$ is the Pauli blocking term.

The Pauli blocking term has been investigated in [4, 20]. It is the main medium effect describing the dissolving of clusters when the density of the nuclear matter reaches the Mott density.

5.1.2. RELATIVISTIC MEAN-FIELD MODEL(RMF)

Relativistic approaches are characterized by Lorentz covariance which constrains the form of the interaction. The spin and spin-orbit interactions are naturally included and at high density the Fermi momentum of the nucleons is high so the relativistic effect is important [1].

Conventional relativistic mean field (RMF) treats nucleons as quasi-particles; their self energy depends on medium proprieties. Nucleons interact by the exchange of mesons (σ, ω and ρ). Nucleons are represented by Dirac spinors and mesons with Lorentz vector.

In the Generalized RMF model the RMF model is extended to include clusters which are treated as point particles and their internal structure is not taken into account. The medium effect on clusters properties is described by density and temperature dependent shifts of binding energy.

5.1.3. VIRIAL EXPANSION

The virial expansion is based on two main assumptions: first the system is in the gas phase and does not change to another phase by changing temperature or density. The second assumption is that the fugacity ($z = e^{\frac{\mu}{T}}$) is small which is satisfied at low densities and not too low temperatures, so the partition function can be expanded   in powers of z.

The virial expansion is considered as extension of the NSE model by including the scattering states in addition to the bound states [1].

5.1.4. NUCLEAR STATISTICAL EQUILIBEUIM MODEL

Nuclear statistical equilibrium model (NSE) is the simplest model for describing nuclear matter at low density. It treats nuclear matter from a statistical point of view as a system of non-interacting or minimally interacting particles at statistical equilibrium. Only the bound states are considered in this model while the excited and scattered states are ignored [4] [10].

5.2. ORIGINAL FORM OF THE NSE MODEL

In the NSE model nuclear matter at low density limit consists of protons (p), neutrons (n) and clusters (X). The interactions between nucleons are neglected in this model; the nucleons only interact by forming clusters. These clusters are formed to minimize the energy and the entropy of the nuclear matter at densities

much less than the saturation density [2-4].The mass number of each cluster is $A=N+Z$. The NSE model assumes that the clusters are in chemical equilibrium with the nucleons in the surrounding vapor. So the nuclear matter obeys the equation below [18]:

$$Zp + Nn \leftrightarrow {}_{Z}^{A}X \tag{5.2}$$

In order to achieve the objectives of this research, we use a modified form of the NSE model. We start from the equation of state for an ideal gas composed of free neutrons and protons. Now the chemical potential of a nuclear cluster at chemical equilibrium is given by:

$$\mu_{cluster} = Z\mu_p + N\mu_n \tag{5.3}$$

We assume the nuclear matter is symmetric, so the chemical potentials of protons and neutrons are equal $\mu_p = \mu_n = \mu$ such that:

$$\mu_{cluster} = A\mu \tag{5.4}$$

where $A = N + Z$. μ is the chemical potential for free nucleons which is defined in equation (2.2) in chapter 2. The density of each type of cluster is calculated by numerical integration of the relation:

$$\rho_C = \frac{N}{V} = \frac{g}{(2\pi)^3} \int d^3q\, n_C \tag{5.5}$$

where $g = 2s + 1$ is the spin degeneracy factor of the cluster. The values of g for stable nuclei are shown in Table 5, where s is the ground state nuclear spin. In equation (5.5) n_C is the probability of finding cluster C with the kinetic energy ε_C^0:

$$n_C = \{exp[\beta(\varepsilon_C^0 - \mu_C - B_C)] \pm 1\}^{-1} \qquad (5.6)$$

where the (+) sign is used for fermionic clusters, while the (-) sign is used for bosonic clusters and B_C is the density-dependent binding energy of the cluster when embedded in the vapor which will be defined in the next section. NSE in its original form substitutes $B_C = B_0$ which is the binding energy of the cluster at zero density. The values of B_0 for various clusters are also shown in Table 5. As the NSE model neglects all the interactions between nucleons and also neglects the medium modification. Therefore in it is original form it predicts that most of the nucleons in symmetric nuclear matter would be bound into clusters [4]. In this work, we will not use NSE model in it is original form. We will modify the NSE model in the next section and we will use the modified form. Also to avoid the overestimation in the deuteron abundance, we rely on the formula in [19] for q^{Mott}. The formula which determine the q^{Mott} (in fm^{-1}) for deuteron is a function of the temperature T and the total nuclear density ρ_{total} .

$$q^{Mott}(T,\rho_{total}) = \sqrt{\frac{\frac{4.5185-0.16164T+0.0056582T^2}{2(1.32-0.02782T)}+}{(\frac{(4.5185-0.16164T+0.0056582T^2)^2}{4(1.32-0.02782T)^2}+\frac{1000(\rho_{total}-\rho_{Mott})}{1.32-0.02782T})^{1/2}}} \qquad (5.9)$$

The values of the Mott densities (ρ_{Mott}) for deuteron which are used in the above equation are illustrated in Table4 at various temperatures. In our calculation the integration limits of the equation (5.5) start from q^{Mott} to ∞ for deuteron density determination.

In this work, we avoid the overestimation of the deuterons by integrating equation (5.5) for deuterons at the region $q > q^{Mott}$ where the bound state energy is lower than continuum of scattering states. This correction has its importance at increasing temperature for weakly bound cluster. It is important for deuterons when the temperature is large or comparable to the binding energy per nucleon [4]. So to avoid this overestimation the integration of the deuteron density must start from q^{Mott} this will eliminate the overestimation of the deuterons as we see in next section in Fig5.20 (the blue circles).

Table 5: Shows the binding energy, mass, experimental values of spin and spin degeneracy of the nuclei used in the current calculation.

Cluster	B_0 (MeV)	Mass(MeV/c^2)	Spin(experimental)	g
^{2}H	2.224560	1876.12	1	3
^{3}H	8.481798	2809.43	½	2
^{3}He	7.718043	2809.41	½	2
^{4}He	28.295660	3728.40	0	1
^{5}He	27.405	4711.48680	3/2	4
^{6}Li	31.99407	5654.2154273	1	3
^{7}Li	39.244037	6595.044277	3/2	4
^{8}Be	56.49948	7524.986794	0	1
^{9}Be	58.47939	8471.451268	3/2	4
^{10}B	64.7507	9412.160780	3	7
^{11}B	76.20481	10348.747076	3/2	4
^{12}C	92.161728	11280	0	1
^{13}C	97.108037	12223.153547532	½	2
^{14}N	104.658596	13162.889564512	1	3
^{15}N	115.491885	14100.102364308	½	2
^{16}O	127.619296	15035.2197423864	0	1
^{17}O	131.762427	15979.183798	5/2	6
^{18}O	137.36889	16920.881720	0	1
^{19}F	147.801285	17858.4990268	½	2
^{20}Ne	160.6448	18792.893764876	0	1
^{21}Ne	167.405973	19734.2158792	3/2	4
^{22}Ne	177.77023	20671.90200716	0	1
^{23}Na	186.564339	21610.383124046	3/2	4
^{24}Mg	198.257016	22545.939198	0	1
^{25}Mg	205.5876	23486.6867048	5/2	6

5.3. THE MODIFIED FORM OF THE NSE MODEL

The original form of the NSE model assumes that nucleons interact by forming clusters only and neglects other interactions. Also NSE model cannot describe the dissolution of clusters with increasing density. To reduce this deficiency in the NSE model, we include the medium effects mainly the Pauli blocking effect by modifying the binding energy of the clusters. We supposed the binding energy of each cluster depending linearly on the total density. The binding energy will be in this form:

$$B_C = B_0(1 - \frac{\rho_{total}}{\rho_{mott}}) \tag{5.7}$$

where ρ_{total} is the total vapor density. B_0 is the cluster binding energy at zero density. ρ_{mott} is the Mott density for the cluster at zero center of mass momentum. The values of the Mott density at different temperatures for each cluster with mass number $2 \leq A \leq 4$ are illustrated in Table 4. For clusters with mass number $A \leq 4$, we have extrapolated their values from the quadratic fit of the known values (Mott densities for clusters up to A=4).

We note from the supposed form of the binding energy of each cluster equation (5.7) the binding energy will return as it is in the original form as the medium density reaches to zero. Also when the density of the medium reaches the Mott density for each cluster its binding energy will be zero. By this modification, we include the decrease in the cluster binding energy as the density of nuclear matter increases. The binding energy of a cluster approaches zero as the density of the nuclear matter approaches the Mott density for that cluster.

To calculate the abundance of each type of cluster, we use the supposed form in equation (5.7) for the binding energy of the clusters, which is a function of the total density (which is not known till now) and represents the final output. To do this many iterations were done to get the final total density as the same total density, we put it in the binding energy of clusters with maximum error (0.5%), then, we use the total density to determine the fraction of each type of clusters. The fraction of nucleons existing in each type of clusters can be evaluated:

$$X_c = A \frac{\rho_c}{\rho_{total}} \qquad (5.8)$$

Once we have the fraction of each type of cluster, we can study their effect in the vapor equation of state. At first, we perform the calculations of the abundances of clusters by including alpha, triton, helion and deuteron to compare our result with the result obtained in [4]. We plot the fraction of each cluster versus the total density at temperatures $T = 6MeV$ and $T = 8MeV$ as shown in Fig.5.1 and Fig.5.2. In the same figures, we plot the Typel results for the fraction of each cluster at temperatures $T = 6MeV$ and $T = 8MeV$.
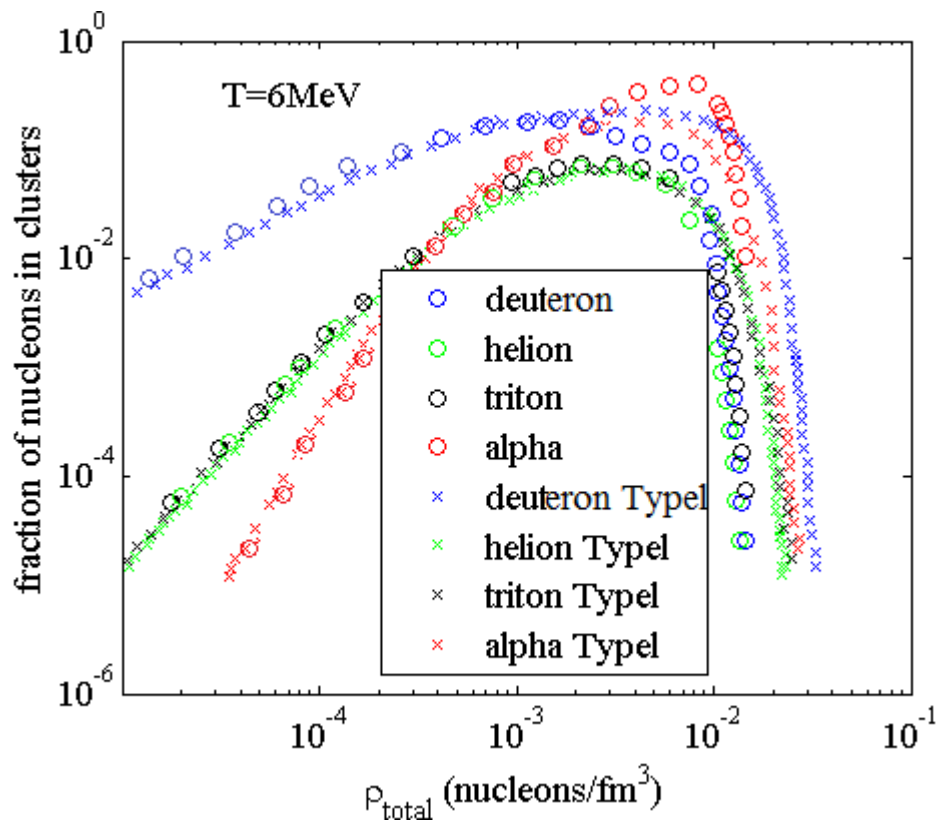
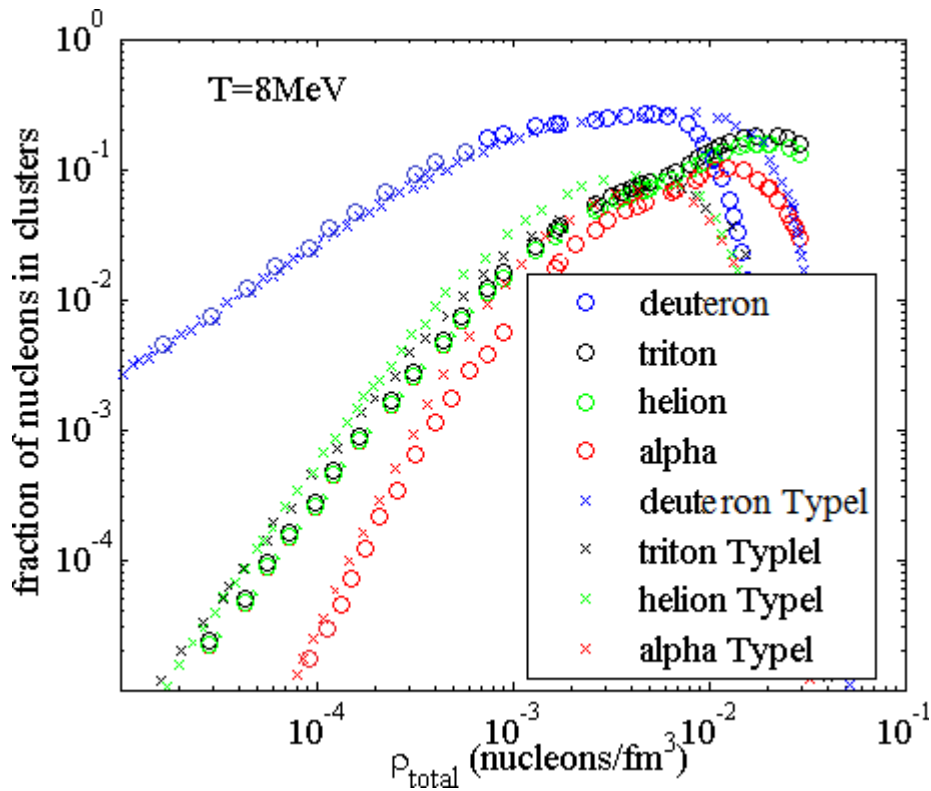**Fig.5.1.** Comparison between the result of this work when including clusters up to A=4 and the Typel result at T=6MeV.

As seen in Fig.5.1 at temperature T=6MeV deuterons, helions and tritons dissolve faster in this work than they do in Typel's work whereas alphas dissolve faster in Typel's work. There is total agreement between Typel results and the results in this work up to densities $\rho \leq 10^{-3} nucleons / fm^3$ (in logarithmic scale) which is equivalent to $\rho = 0.002 \ nucleons / fm^3$.

Fig.5.2. Comparison between the result of this work when including clusters up to A=4 and the Typel result at T=8MeV.

The result in [4] is based on the generalized RMF model. The results in this work are based on the modified NSE model. As we noticed there is agreement between the two models until the total density of nuclear matter approaches 10^{-2} $nucleons/fm^3$. Above this density there is a difference between the two models where in this region the effect of Pauli principle appear which is introduced in different formula in each of the models. From Fig.5.1 and Fig.5.2 we see that the clusters in the modified NSE model start to dissolve at densities higher than densities which dissolve at it in RMF model and this is more pronounced at temperature $T = 8MeV$. But this does not include deuterons which dissolve faster at the two temperatures in the modified NSE model because we

excluded the overestimation in the deuteron abundance by integrate equation (5.5) from q^{Mott} to ∞ to avoid the space region where the bound state do not exit. Now, let us demonstrate the abundances of clusters with mass number $5 \leq A \leq 25$ at temperatures $T = 4MeV$ and $T = 6MeV$.
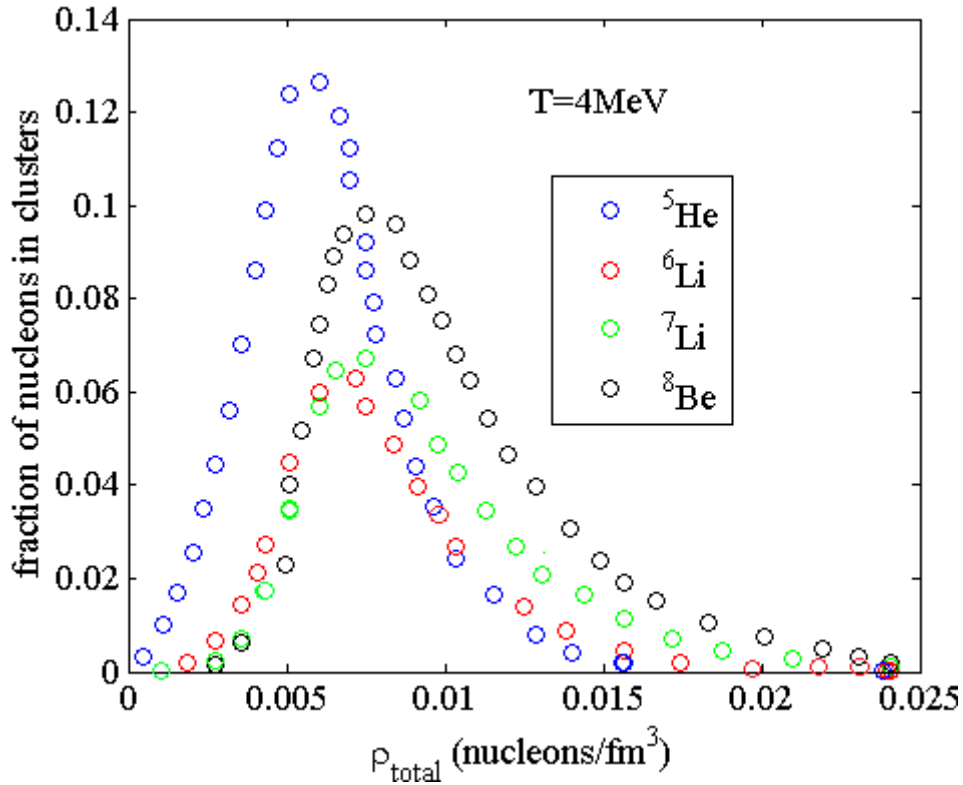
Fig.5.3. The fractions of nucleons in clusters which have $5 \leq A \leq 8$ at T=4MeV.

We see in Fig.5.3 the abundances of various clusters which have mass number $5 \leq A \leq 8$ at temperature $T = 4MeV$. The abundance of each cluster reaches to (6.5% - 13%) from the total abundance at densities $\rho < 0.01\ nucleons/fm^3$. For heavier clusters with mass number $9 \leq A \leq 14$ the abundance of each cluster reaches to (7% -11%) at densities $\rho < 0.015\ nucleons/fm^3$, we can see that in Fig.5.4.
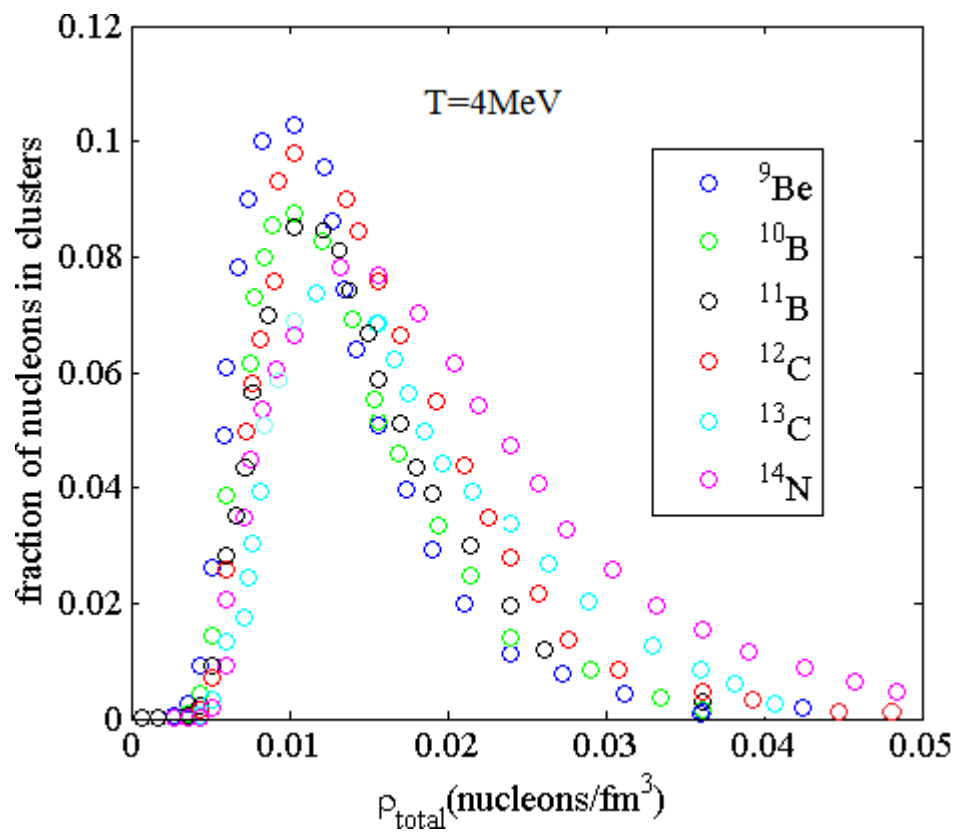
Fig.5.4. The fractions of nucleons in clusters which have **9 ≤ A ≤ 14** at T=4MeV.
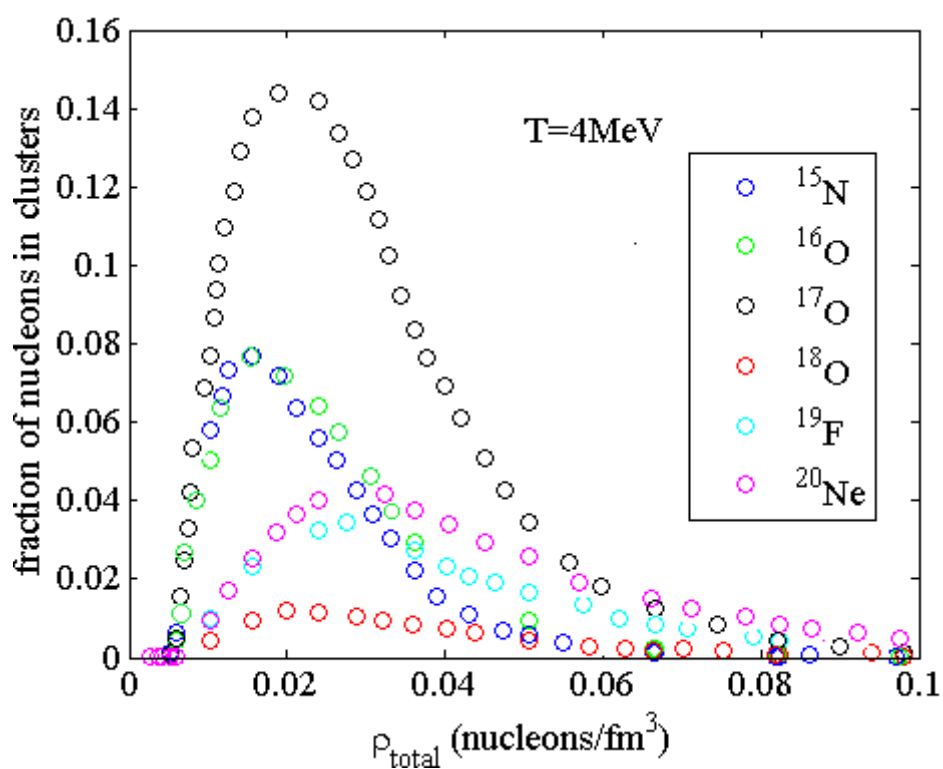
Fig.5.5. The fractions of nucleons in clusters which have $15 \leq A \leq 20$ at T=4MeV.
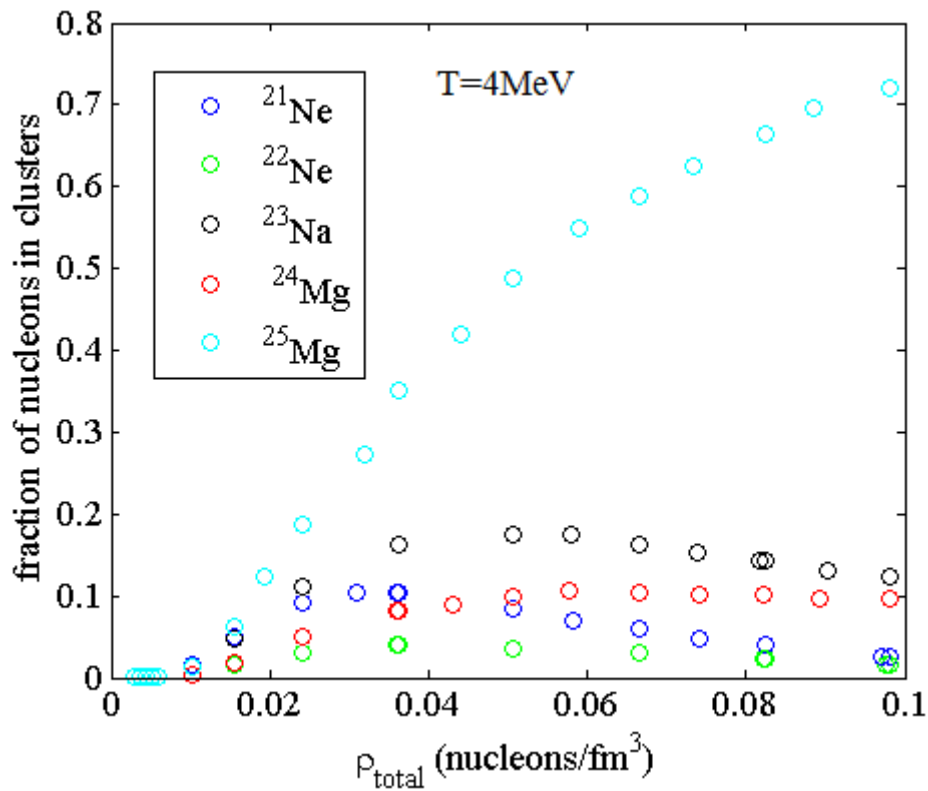
Fig.5.6. The fractions of nucleons in clusters which have $20 \leq A \leq 25$ at T=4MeV.

For clusters with mass number $15 \leq A \leq 20$ the abundance of each cluster reaches to (1% -14%) as seen in Fig.5.5. We can note from Fig.5.6 the abundances of clusters which have mass number $20 \leq A \leq 25$ at temperature $T = 4MeV$ appear strongly at densities $\rho > 0.02 \, nucleons/fm^3$. The abundances of (^{21}Ne, ^{22}Ne, ^{23}Na and ^{24}Mg) change from 2% to 18%. Whereas the abundance of ^{25}Mg increases with density increasing this reflects the importance of including heavier clusters at low temperature.
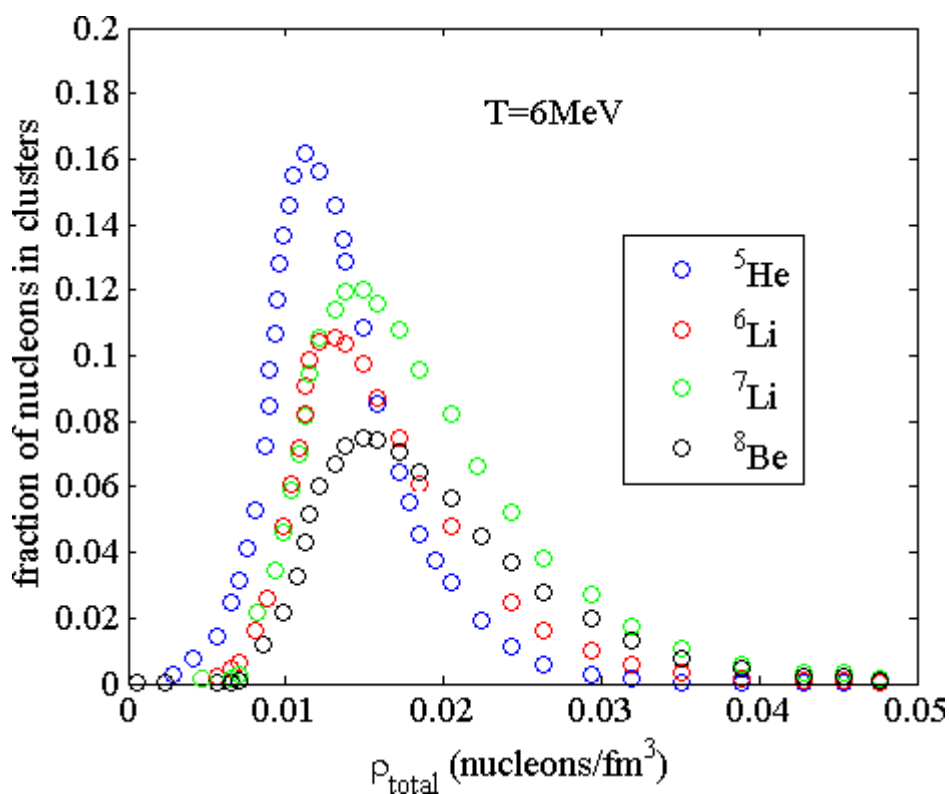
Fig.5.7. The fractions of nucleons in clusters which have $5 \leq A \leq 8$ at temperature T=6MeV.

We see in Fig.5.7 that at low nuclear density $\rho \leq 0.02 \, nucleons/fm^3$ at temperature T=6MeV the clusters which have a mass number $5 \leq A \leq 8$ are

formed with abundance above 16% for ^{5}He. Also the abundances of ^{6}Li and ^{7}Li reach to the values higher than the values at temperature $T = 4MeV$. Whereas the abundance of ^{8}Be has less value in comparison with it is value at temperature T=4MeV. These clusters start to dissolve at densities above $\rho = 0.01\ nucleons/fm^{3}$. Whereas in Fig.5.8 heavier clusters which have $9 \leq A \leq 14$ start to dissolve at densities $\rho \geq 0.02\ nucleons/fm^{3}$.
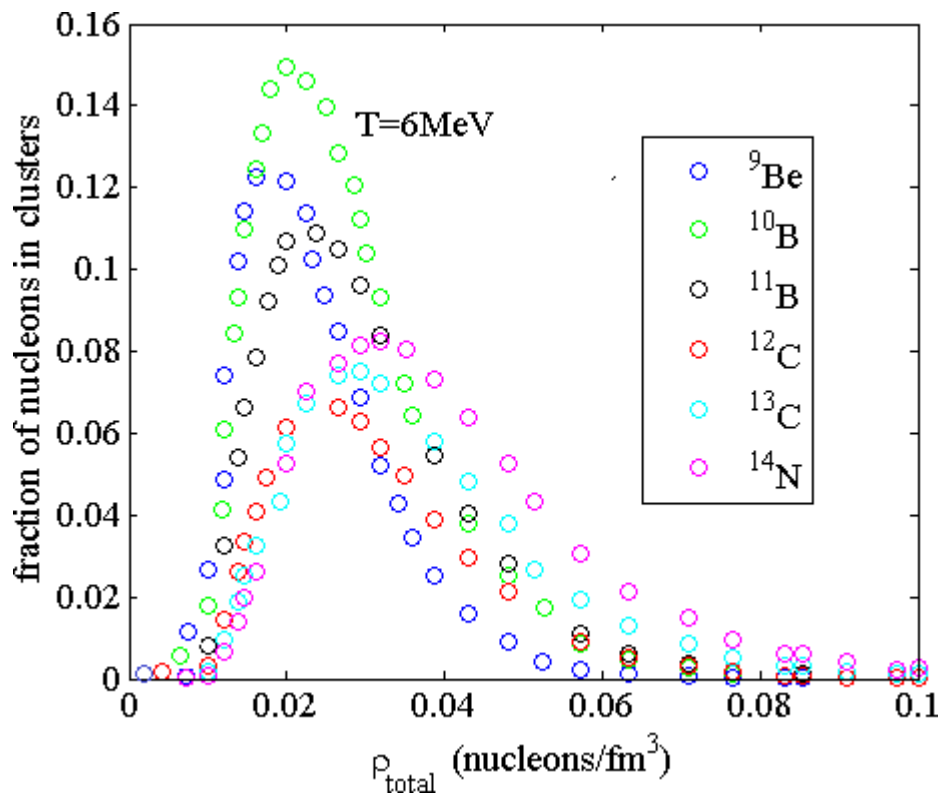

Fig.5.8. The fractions of nucleons in clusters which have $\mathbf{9 \leq A \leq 14}$ at temperature T=6MeV.

We can note from Fig.5.7 and Fig.5.8 the lighter clusters start to dissolve faster than the heavier one. The abundance reaches to 11% at density $\rho \cong 0.03\ nucleons/fm^{3}$ for ^{10}B. In Fig.5.9 the abundance of ^{17}O reaches to 17%

and the clusters which have a mass number $15 \leq A \leq 20$ start to dissolve at density $\rho \cong 0.05 \ nucleons/fm^3$.

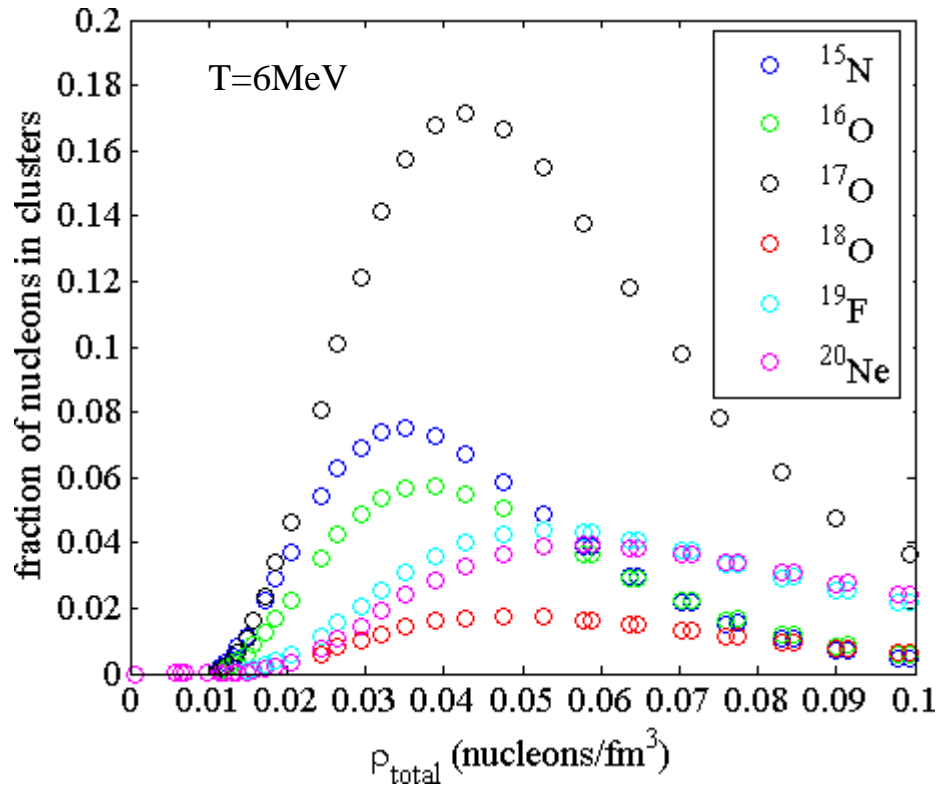**Fig.5.9.** The fractions of nucleons in clusters which have $\mathbf{15 \leq A \leq 20}$ at temperature T=6MeV.

We see in Fig.5.10 the clusters which have a mass number $21 \leq A \leq 25$ appear significantly at densities above $\rho = 0.06 \ nucleons/fm^3$. And at low density these clusters give negligible contribution in the total abundance. These clusters give significant contribution in the total abundance of clusters at high density which is not our subject also NSE model fails in high density limit.
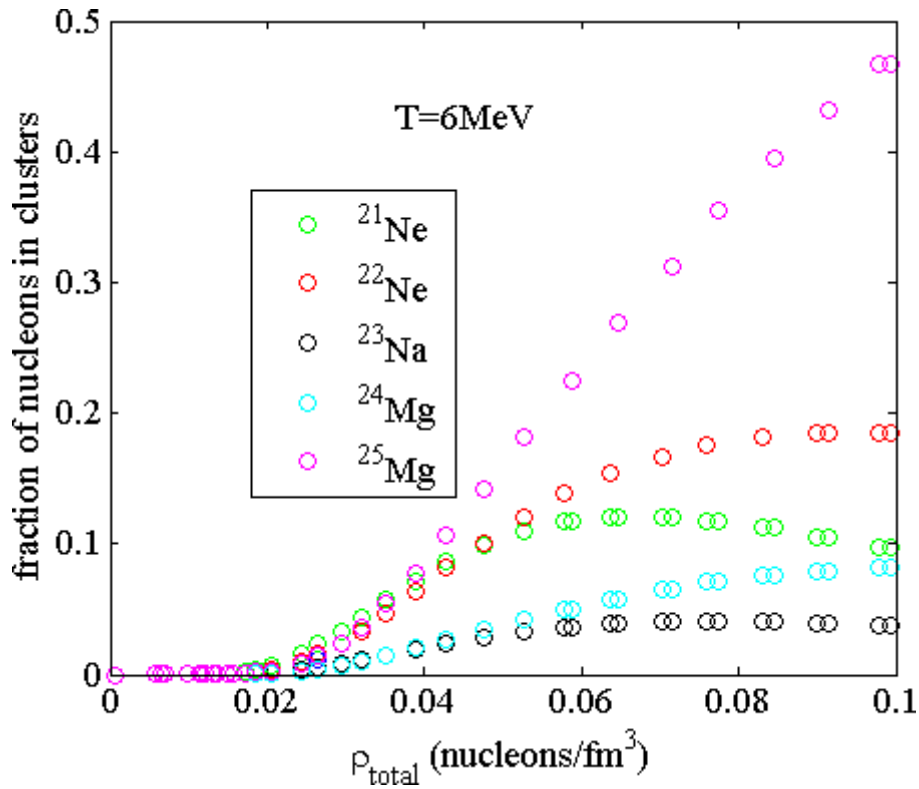
Fig.5.10. The fractions of nucleons in clusters which have $21 \leq A \leq 25$ at temperature T=6MeV.

From the investigation (Fig.5.3-Fig.5.10) for the abundances of the clusters with mass number $5 \leq A \leq 25$ at temperature $T = 4MeV$ and $T = 6MeV$, we can say that the abundances of these clusters have significant contribution in the total abundance. The previous studies [4, 6, 11, 20] included alphas, helions, tritons and deuterons only in addition to free nucleons. But in this work, we proof that the clusters with mass number $5 \leq A \leq 25$ have a contribution cannot be neglected at different density ranges. In Fig.5.11 and Fig.5.12, we compare the abundances of clusters with mass number $5 \leq A \leq 25$ with clusters with A=2-4 at temperature $T = 6MeV$.

We found that the deuterons are still dominant at very low density as in [4]. Then

tritons, helions and alphas appear respectively (as seen in Fig.5.11) ; this occur at

densities $\rho < 0.01 \; nucleons/fm^3$ but at higher densities the abundances of

clusters have A>4 is sizable. As we can see in Fig.5.12 these clusters appear

strongly at densities $\rho < 0.02 \; nucleons/fm^3$ and above this density the clusters
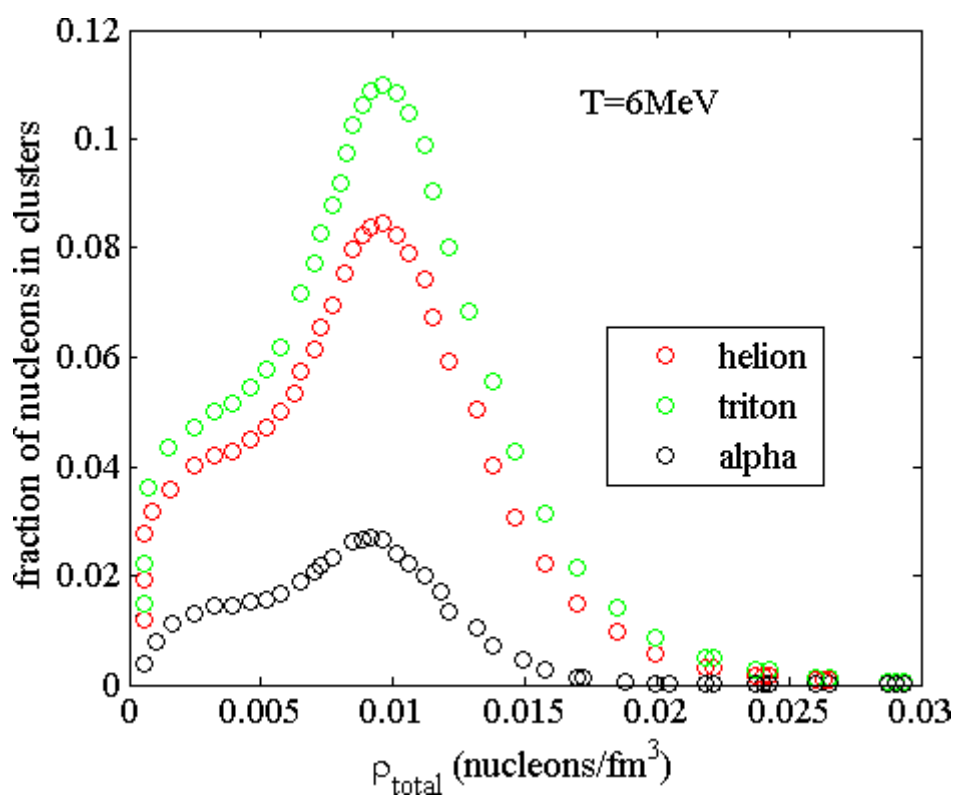
with mass number $5 \leq A \leq 25$ are the dominant.

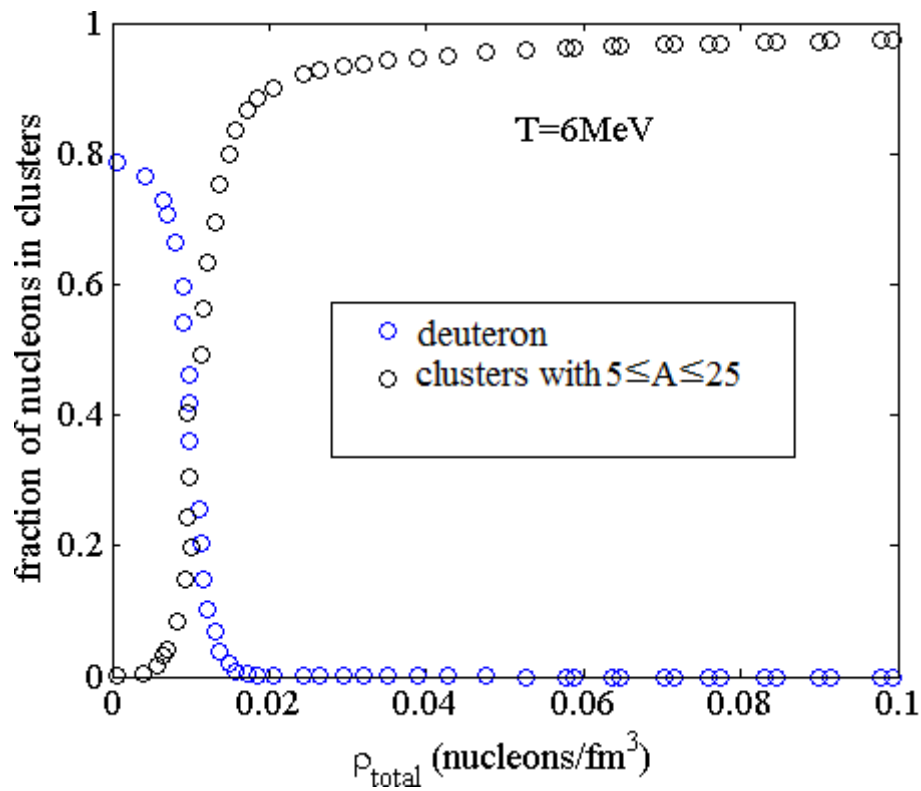**Fig.5.11.** The abundances of hellion, triton and alpha particles at T=6MeV.

Fig0.5.12. The abundances of deuteron and all the clusters with mass number $5 \leq A \leq 25$ at T=6MeV

We note from the previous figures that the abundances of clusters change with density. But also the composition of nuclear matter is affected by the temperature as the Pauli effect is less effective at higher temperature [4].We should investigate the abundances for the same clusters at different temperatures. So we pick six clusters which are most of the time the most abundant in their mass range. We demonstrate the abundances of the picked clusters which are (deuterons, alpha, ^{7}Li, ^{10}B, ^{17}O, and ^{25}Mg) at temperatures $2MeV \leq T \leq 12MeV$.

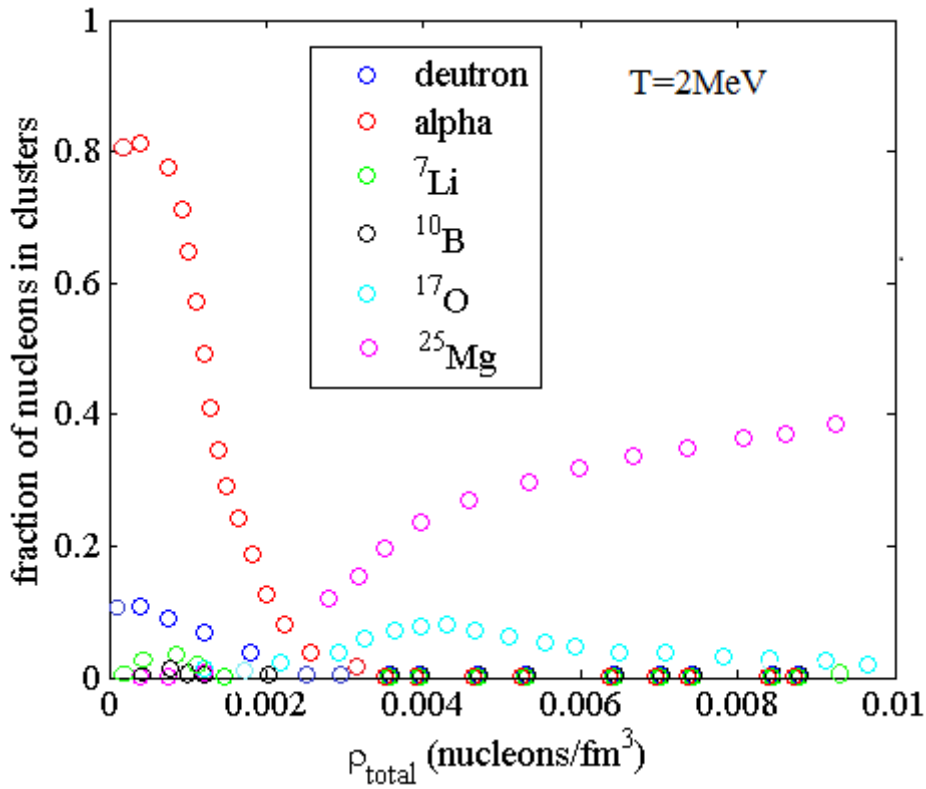**Fig.5.13.** The fraction of nucleons in clusters at T=2MeV

We note from Fig.5.13 Alpha particles are dominant at very low densities $\rho < 0.003\ nucleons/fm^3$ and at temperature $T = 2MeV$ .The deuterons abundance is above 10% at densities $\rho < 0.005\ nucleons/fm^3$. While the abundances of ^{7}Li and ^{10}B give small contribution at low density $\rho < 0.002\ nucleons/fm^3$. The abundance of ^{25}Mg is large even at low density $\rho < 0.004\ nucleons/fm^3$ at temperature $T = 2MeV$ also the abundance of O^{17} reaches to 9% at low density. This reflects significant contribution for heavier clusters especially at densities above $\rho \leq 0.004\ nucleons/fm^3$ at temperature $T = 2MeV$.
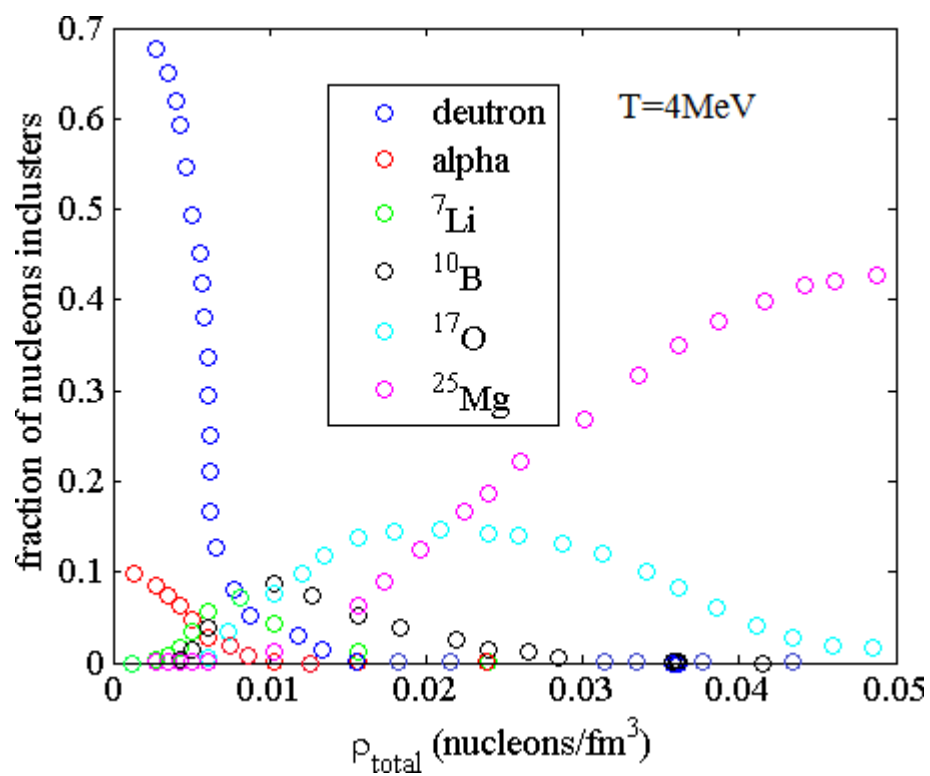
Fig.5.14. The fractions of nucleons in clusters at T=4MeV

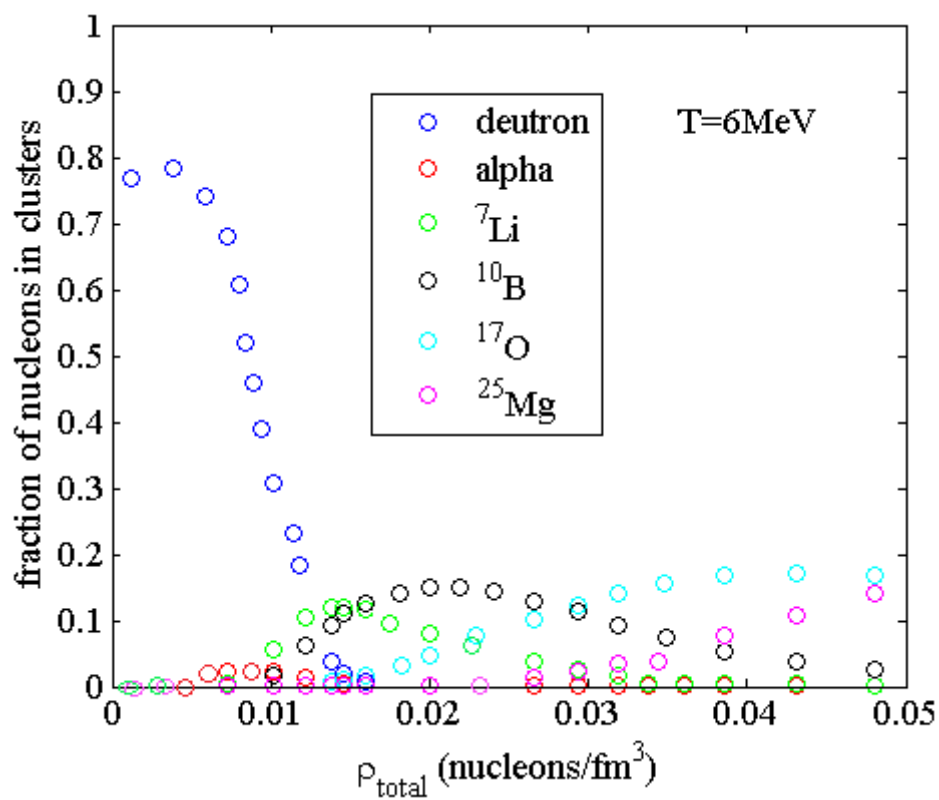**Fig.5.15.** The fractions of nucleons in clusters at T=6MeV

We can note from Fig5.14 and Fig.15 the abundances of ^{7}Li, ^{10}B and ^{17}O appear more strongly at higher temperatures $T = 4MeV$ and $T = 6MeV$, whereas they have small contributions at temperature $T = 2MeV$ as illustrated in Fig5.13.
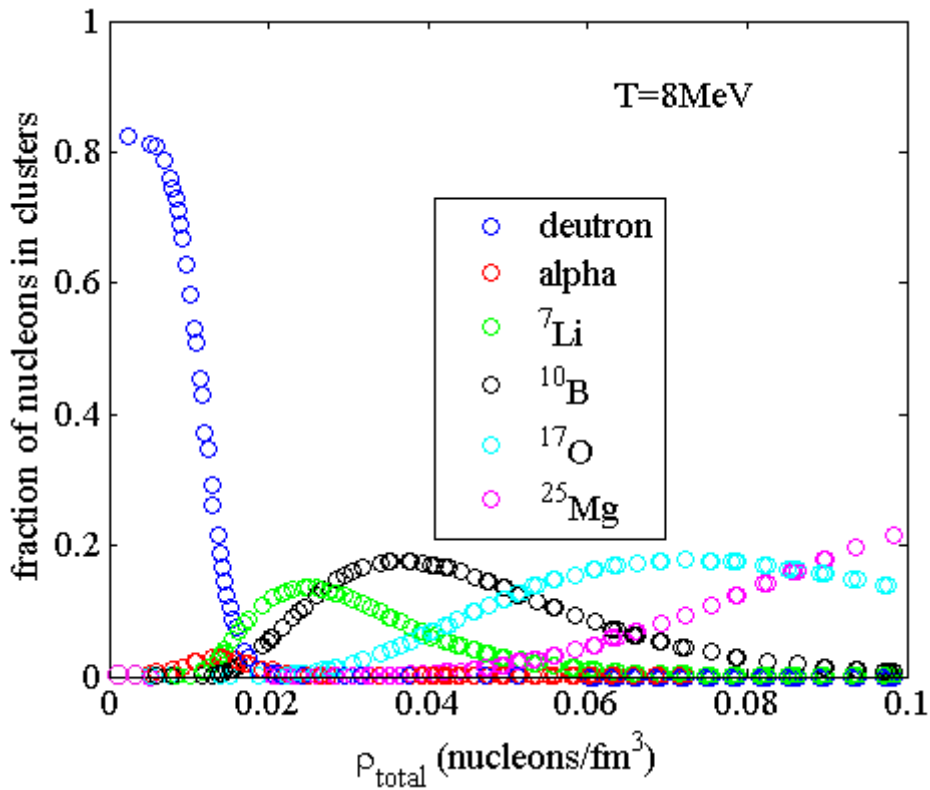
Fig.5.16. The fractions of nucleons in clusters at T=8MeV

In Fig.5.14 and Fig.5.15, we note that deuterons dissolve at low density $\rho < 0.01\ nucleons/fm^3$ at temperatures $T = 4MeV$ and $T = 6MeV$. Whereas in the case of the temperature $T = 8MeV$ deuterons survive at higher density up to $\rho = 0.02\ nucleons/fm^3$ at as shown in Fig.5.16. ^{7}Li and ^{10}B appear at temperature $T = 4MeV$ at densities $0.005 \leq \rho \leq 0.015\ nucleons/fm^3$ while ^{17}O and ^{25}Mg appear strongly at densities $\rho \leq 0.02\ nucleons/fm^3$. Whereas at temperature $T = 6MeV$ the heavier clusters (^{17}O and ^{25}Mg) appear strongly at densities $\rho \leq 0.03\ nucleons/fm^3$. At temperature $T = 8MeV$ ^{7}Li and ^{10}B appear strongly at densities $0.02 \leq \rho \leq 0.04\ nucleons/fm^3$ the heavier clusters (^{17}O and ^{25}Mg) appear strongly at densities $\rho \geq 0.05\ nucleons/fm^3$. At higher

temperatures $T = 10MeV$ and $T = 12MeV$, we note that the heavier clusters appear at densities $\rho \geq 0.06\ nucleons/fm^3$ while the deuterons survive above this density.
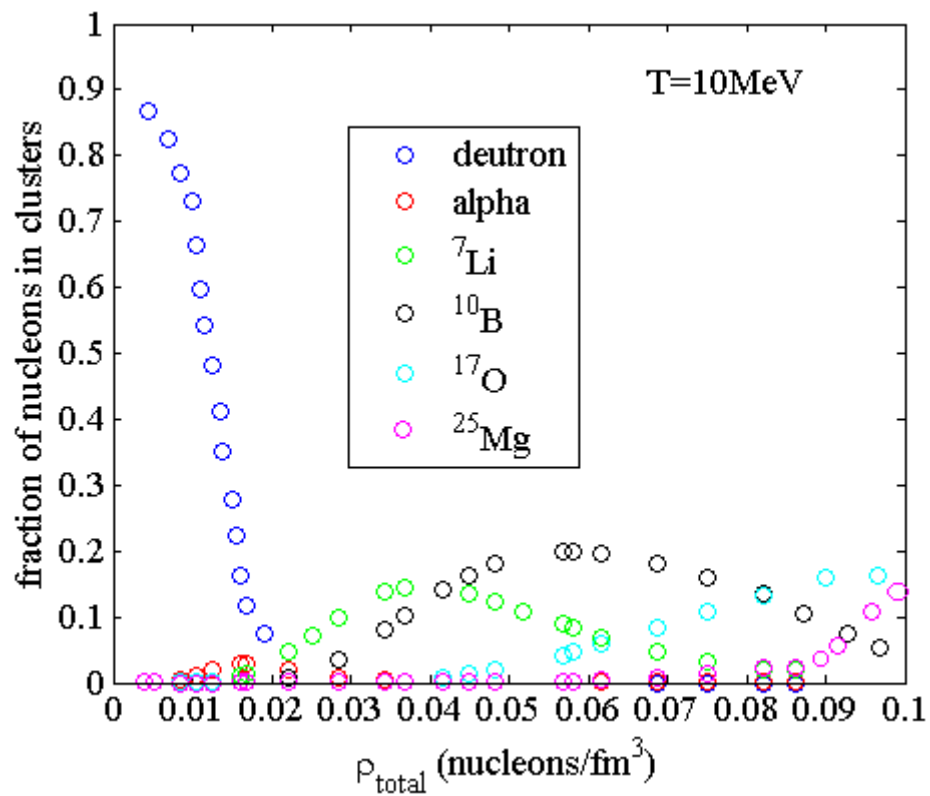

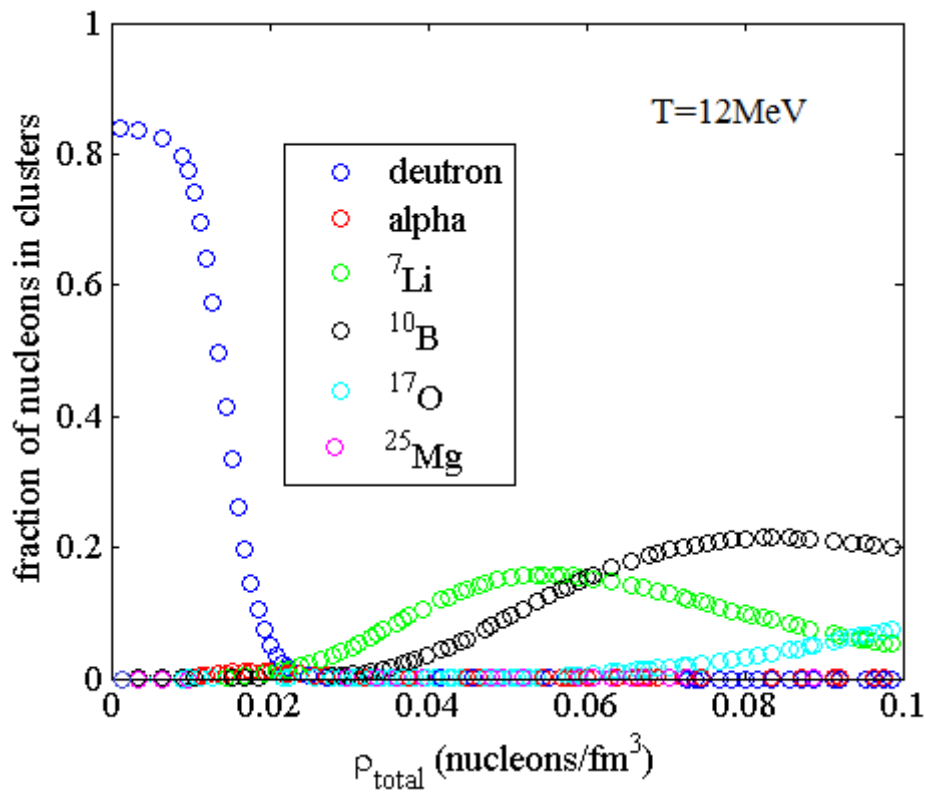**Fig.5.17.** The fractions of nucleons in clusters at T=10MeV

Fig.5.18. The fractions of nucleons in clusters at T=12MeV

We can note from Fig.17 and Fig.18 that the abundances of the heavier clusters give less contribution by temperature increasing at the same density limit. The heavier clusters have a significant contribution at temperatures $2MeV \leq T \leq 8MeV$. The abundances of these clusters change as the temperature changes; the heavier clusters appear at higher densities with temperature increasing.

We can note that deuterons are dominant at very low density except in the case of very low temperatures ($T <= 2MeV$) where the alphas are dominant. Deuterons dissolve faster at low temperature and with temperature increasing survive to higher densities. As shown in Fig.5.19 most of the nucleons bound to deuterons and alphas at very low density and temperature. This emphasized the

result in [13] and at higher density at the same temperature the deuteron abundance will be larger than the alpha's abundance.
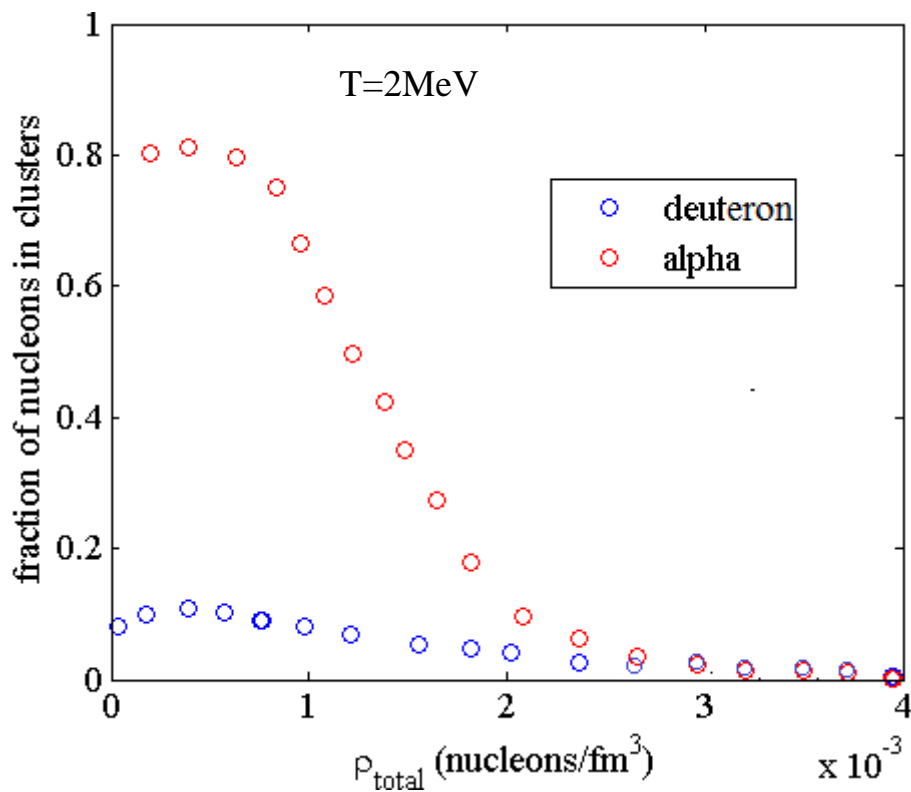

Fig.5.19. The fractions of nucleons in clusters at T=2MeV

Before leaving chapter 5, we must discuss the overestimation in the deuteron abundance which appears strongly with temperature increasing at higher density. We discussed the determination of the density for each cluster in section5.2. By using the integration in equation (5.5) as it is in original form (as q changes from zero to infinity) the overestimation will appear strongly. Because in this case the integration is over the entire of the momentum space which means the region where the bound states do not exist are included as illustrated in Fig.5.20 the result for deuteron abundance at temperature $T = 12\ MeV$ (red circles).
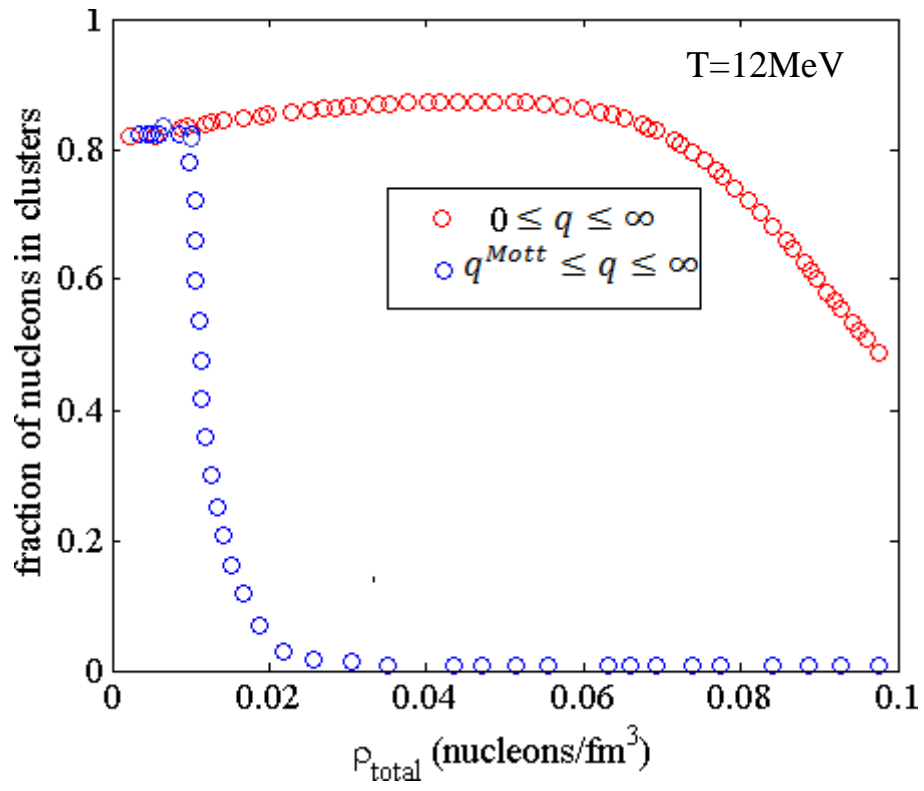
Fig.5.20. The abundance of deuteron at T=12MeV in two cases once with including all the momentum space (red circles) and other with including the region $q > q^{Mott}$ (blue circles).

CHAPTER6. RESULTS AND CONCLUSIONS

In chapter 5, we calculated the density of each type of clusters; also we demonstrated the abundances of these clusters. As we have the density of each type of clusters, we can calculate the partial pressure for each type of clusters and nucleons using the ideal Fermi and Bose equations of state. In this chapter, we will study the effect of including clusters up to A=25 on critical point and compare it by previous results mainly in [13].

6.1. EQUATION OF STATE OF CLUSTERED NUCLEAR MATTER

Now, we can determine the pressure equation of state by summing the pressure of free nucleons and the partial pressure of each cluster:

$$P = P_{free} + P_{clusters} \qquad (6.1)$$

where P_{free} is the pressure of free nucleons (ideal Fermi equation of state) which is defined in chapter 2 (equation (2.3)) and $P_{clusters}$ is the total pressure of all the clusters which is determined by ideal Fermi and Bose equations which are defined in chapter 2 (equation (2.6) and equation(2.3)). In Fig.6.1, we plot the pressure isotherm at temperature $T = 10MeV$ for ideal gas of nucleons using equation (2.3). Also in the same figure, we plot the pressure isotherm for a system of interacting nucleons via Skyrme interactions using equation (3.10) and the pressure isotherm for clustered nuclear matter using equation (6.1).
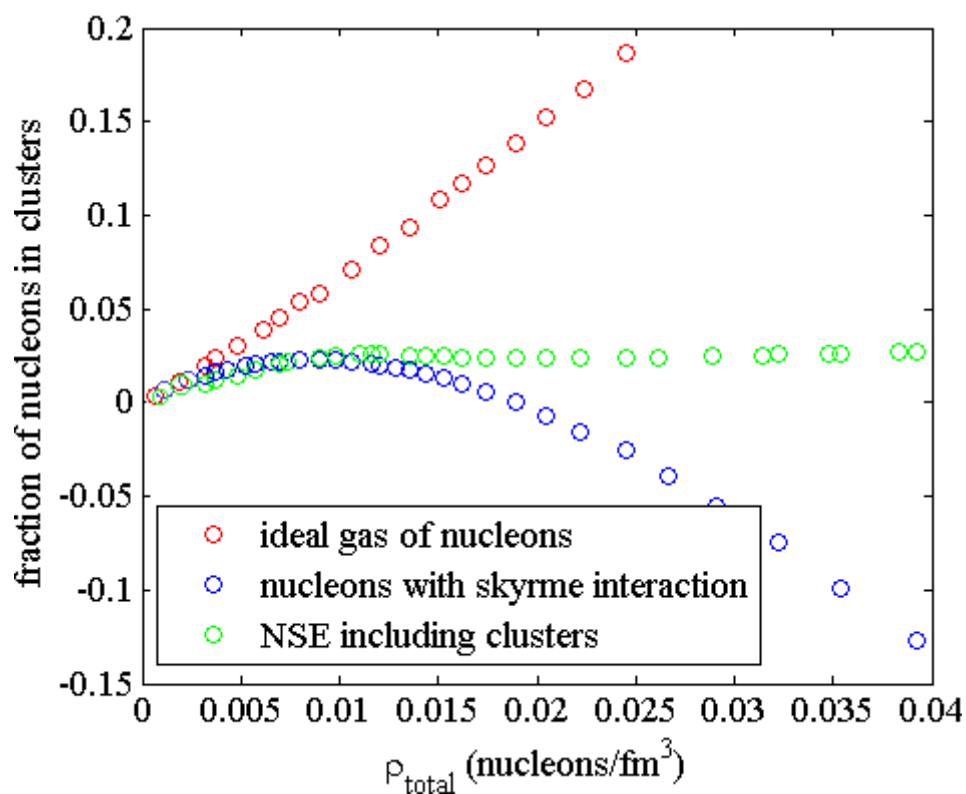
Fig.6.1. Comparison between ideal gas of nucleons, nucleons interacting via Skyrrme force and the nuclear matter in nuclear statistical equilibrium model at T=6MeV.

In Fig.6.1 the pressure isotherm of free nucleons behaves as ideal gas at low density. In the same figure the pressure isotherm of nucleons interacting via the Skyrme force; we can note the values of pressure in this case are less than the values of pressure of free nucleons. Also we note that the values of pressure of clustered nuclear matter are less than the values of the pressure of free nucleon. In the nuclear statistical equilibrium (NSE) model the nucleons interact by forming clusters.

In chapter 3, we determined the critical temperature for nucleons interacting via the Skyrme force. In this chapter, we determine the critical temperature for clustered nuclear matter using equation (6.1).
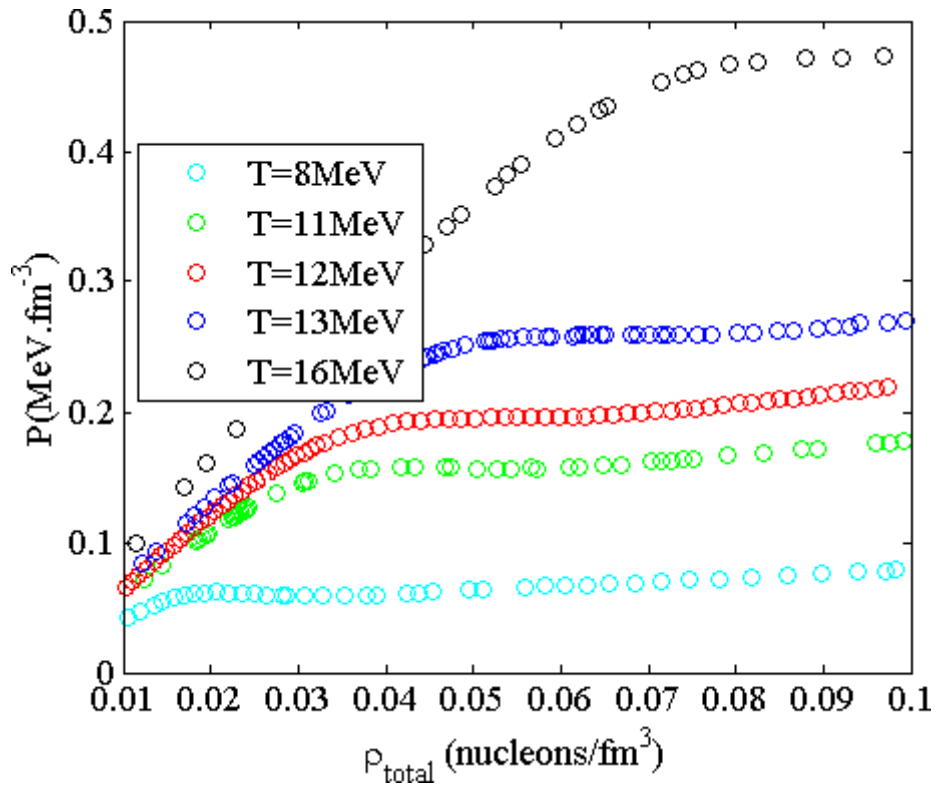
Fig.6.3. The pressure isotherms for clustered nuclear matter in the modified NSE model at different temperatures.

It is seen from the above figure the behaviour of the pressure isotherms for clustered nuclear matter change with temperature. We can note that the critical temperature will be between $T = 11 MeV$ and $T = 13\ MeV$. To identify the critical temperature, we plot the pressure isotherms at close temperatures in the region that, we expected the existence of critical temperature in Fig.6.3.
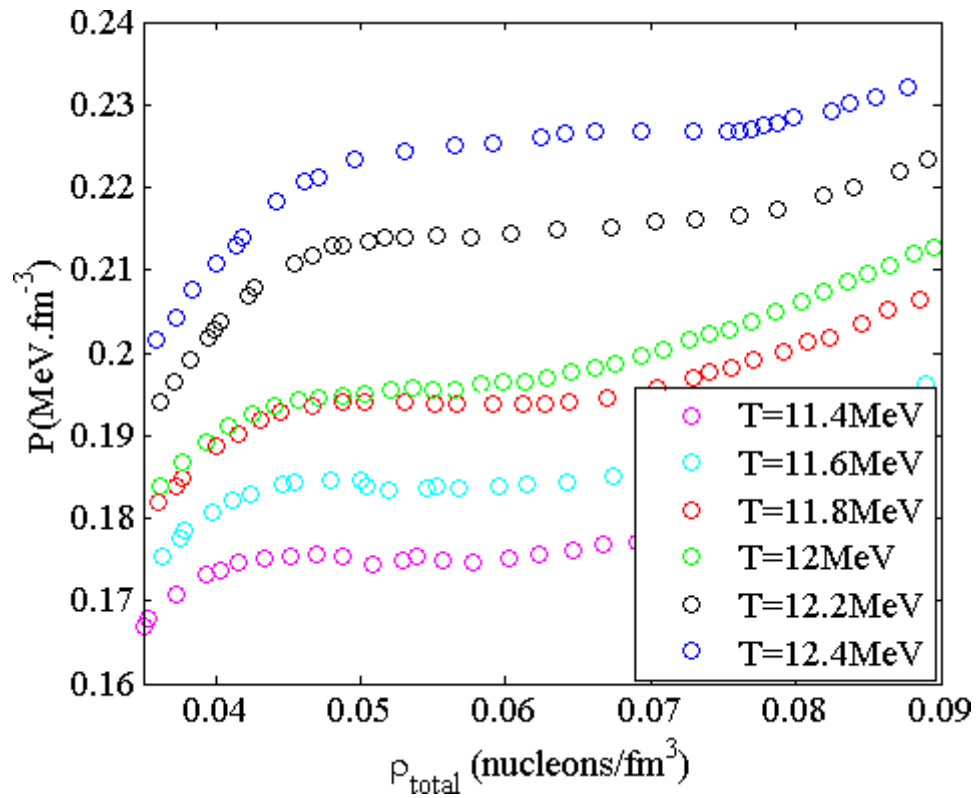
Fig.6.3. The critical temperature from the pressure isotherms for clustered nuclear matter in the modified NSE model.

From the above figure, we note that the critical temperature is $T = 11.8 MeV$. We summarize the critical point (temperature, pressure and density) for clustered nuclear matter using modified NSE model in Table6.

Table 6: Comparison the value of the critical point in [13] and in this work

	$T_{critical}$ MeV	$\rho_{critical}$ $nucleons/fm^3$	$P_{critical}$ $MeV.fm^{-3}$
In this work	11.8	0.06	0.0194
In [13] $\sigma = 0.25$	17.3	0.0535	0.2745

Under the critical temperature two distinct phases coexist (a dense liquid phase and a dilute gaseous phase) whereas above this temperature only one fluid phase can exit. The difference between the result in [13] and in this work is not just due to using different models. In [13] the Skyrme interaction between nucleons is considered and the formation of clusters is neglected. In this work, we used modified formula of the NSE model and the formation of clusters up to $A = 25$ is considered.

6.2. CONCLUSIONS

We can conclude:

a) Studying formation of the clusters at low density matter must include the clusters with mass number $A > 4$. The appearance of the clusters with mass number $5 \leq A \leq 8$ at temperature $T = 4MeV$ is pronounced at densities less than $\rho = 0.01 \ nucleons/fm^3$. At higher temperatures $6MeV \leq T \leq 12MeV$ these clusters appear strongly at densities $0.01 \geq \rho \geq 0.06 \ nucleons/fm^3$.

b) The appearance of clusters with mass number $9 \leq A \leq 14$ is strong at densities $0.01 \leq \rho \leq 0.02 \quad nucleons/fm^3$ at temperature $T = 4MeV$. At higher temperatures $6MeV \leq T \leq 12MeV$ these clusters appear strongly at densities $0.02 \leq \rho \leq 0.1 \ nucleons/fm^3$.

c) The clusters with mass number $15 \leq A \leq 20$ appear at densities $0.02 \leq \rho \leq 0.04 \ nucleons/fm^3$ at temperature $T = 4MeV$. Where at temperatures $6MeV \leq T \leq 12MeV$ these clusters appear strongly at densities $0.02 \geq \rho \geq 0.1 \ nucleons/fm^3$.

d) The clusters with mass number $20 \leq A \leq 25$ appear significantly at densities $\rho > 0.01 \ nucleons/fm^3$ at temperature $T = 2MeV$. Also appear strongly at densities $\rho > 0.02 \ nucleons/fm^3$ at temperatures $T > 2MeV$.

e) The abundances of clusters with mass number $A \leq 25$ reduce the critical temperature by several MeV's.

In this thesis, we determined the abundances of the small and medium sized clusters for infinite symmetric nuclear matter. This nuclear matter consists of free nucleons and bound states of nucleons (clusters) whereas scattering and excited states are neglected. The interactions between nucleons are ignored except through the formation of the clusters. Also the effective masses of the nucleons and the clusters are not considered. Further work may include the interactions between nucleons (such as Coulomb interaction). Medium modifications such as the effective masses of nucleons and clusters may be included.

The determination of the composition of infinite nuclear matter in the low density limit can help in understanding supernova especially the ejected material from the core to the outer layers of the star. In further work, we suggest to study the stability of hot nuclei embedded in the nuclear vapour (as we treated in this thesis) which simulates the case of the stability of the nuclei in the outer layers of star embed in the ejected material (nuclear vapour) from it is core.

REFERENCES:

[1] Typel. S.2013 Clusters in Nuclear Matter and the Equation of State. *IOPscience* 420: 1-16

[2] Beyer, M. Strauss, S. Schuck, P. and Sofianos, S. A. 2004 Light clusters in nuclear matter of finite temperature *European Physical Journal EPJ* 22(2): 261.

[3]Horowitz, C. J. and Schwenck, A. 2006 Cluster formation and the virial equation of state of low-density nuclear matter *Nuclear Physics A* 776(1-2): 55.

[4] Typel. S, Röpke. G, Klähn. K, Blaschke. D, and H. Walter. 2010 Composition and Thermodynamics of nuclear matter with light clusters. *Physical Review C* 81: 1-22.

[5] Röpke, G. Munchow, L. and Schulz, H. 1982 Practical clustering and Mott transition in nuclear matter at finite temperature. I. Method and general aspects *Nuclear Physics A* 379: 536.

[6] Röpke. G, Grico. A, Sumiyoshi. K and H. Shen. 2005 The nuclear matter equation of state including light clusters. *PEPAN letters* 128 (5): 25-36.

[7] Röpke, G. Schmidt, M. Munchow, L. and Schulz H. 1983 Practical clustering and Mott transition in nuclear matter at finite temperature. II. Self-consistent Ladder Hartree-Fock approximation and model calculations for cluster abundances and phase diagram *Nuclear Physics A* 399: 587.

[8] Levit. S and P. Bonche. 1985 Coulomb instability in hot compound nuclei approaching liquid gas transition. *Nuclear Physics A* 437:426-442

[9] Jaqaman, H. R. 1989 Coulomb instability of hot nuclei *Physical Review C* 39(1): 169.

[10] Jaqaman, H. R. 1989 Instability of hot nuclei *Physical Review C* 40(4): 1677.

[11] Sumiyoshi.k and Ropke .G .2008 Appearance of Light Clusters in Post-bounce Evolution of Core-Collapse Supernovae.

[12] Röpke, G. 2009 Light nuclei quasiparticle energy shifts in hot and dense nuclear matter *Physical Review C* 79: 014002.

[13] Talahmeh, S. and Jaqaman, H. R. 2013 Light cluster formation in low density nuclear matter and the stability of hot nuclei *J. Phys. G: Nucl. Part. Phys.* 40: 015103.

[14] Wong, S. 2004 *Introductory nuclear physics* 2nd edition. Weinheim: Wiley-VCH Verlag GmbH & Co. KGaA.

[15] Pathria, R.K and Beale,P.D 2011 *Statistical mechanics* 3rd edition. Elsevier Ltd.

[16] Vautherin, D. and Brink, D. M. 1972 Hartree-Fock calculations with Skyrme's interactions. I. Spherical nuclei. *Physical Review C*, 5(3): 626.

[17] Jaqaman. H. R, Mekjian. A. Z and L. Zamick. 1983 Nuclear Condensation. *Physical Review C 27* (6): 2782 – 2793.

[18] Abdul-Rahman. A, Alstaty. M and Jaqaman. H. R. 2015 Center Of Mass Motion And The Mott Transition In Light Nuclei. Journal Of Physics G.

[19] Röpke, G. 2011 Parametrization of light nuclei quasiparticle energy shifts and composition of warm and dense nuclear matter *Nuclear Physics A* 867: 66.

[20] Röpke. G. 2010 Medium effects and quantum condensates in low density nuclear matter. *Acta Physica Polonica B* 3 (3) 649-685.

[21] Skyrme, T. 1959 The effective nuclear potential *Nuclear Physic* 9(4): 615.

[22]S. Kowalski et al. 2007 Experimental determination of the symmetry energy of a low density nuclear gas. *Physical Review C* 75:014601.